A review on the turbulence modelling strategy for ship hydrodynamic simulations

Blanca Pena and Luofeng Huang*

Department of Mechanical Engineering, University College of London, United Kingdom

Abstract: Ship operations are accompanied by turbulent regimes that play a significant role in the hydrodynamic characteristics of a flow. With the ongoing development of computational technologies, it is now feasible to numerically simulate turbulent ship flows with a high degree of detail. Turbulent simulations, however, tend to be computationally expensive and require a trade off between computational costs and fidelity. Whilst a range of turbulence modelling strategies is available in Computational Fluid Dynamics, there is a lack of up-to-date recommendations on their suitability for different ship flow simulation scenarios. Addressing this gap, the present work reviews the state-of-the-art of turbulence modelling for ship hydrodynamic applications. As a result, this paper introduces the most known turbulence modelling approaches used in ship hydrodynamics, followed by a thorough discussion of their applicabilities and limitations. Furthermore, this paper provides recommendations for the selection of turbulence modelling strategies versus various ship simulation scenarios, such as resistance prediction, ship flow modelling, self-propulsion, and cavitation analyses. It is expected that the present paper will provide decision-making support by helping CFD users minimise the time spent on trial and error, as well as providing valuable insights to promote the advancement of turbulence modelling.

Keywords: Ship, Turbulence, Computational Fluid Dynamics, Reynolds-Average Navier-Stokes, Large-Eddy Simulation, Detached Eddy Simulation.

Corresponding author: ucemlhu@ucl.ac.uk

1. Introduction

Computational fluid dynamics (CFD) is one of the most important approaches used in ship design. From integral ship resistance to local structural response, CFD has been proven to be a legitimate prediction technique. Compared to lab experiments, CFD is much cheaper and can provide much more information about the flow that cannot be captured during experiments. Hereby, it has been a widespread trend in the shipping industry, academia and international societies that designate CFD as an essential skill (ASME, 2009; ITTC, 2014a).

The comprehensive capabilities of CFD provide abundant options on numerical set-ups, bringing many questions on how to make choices. For example, the spatial and temporal discretisation resolutions, known as mesh density and timestep size respectively, play a crucial role in computational accuracies (Jasak et al., 2007). Generally speaking, a higher spatial and temporal resolution can yield more accurate results while the demanded computational recourses to solve a simulation will increase accordingly. Due to this reason, sensitivity tests on mesh/timestep size are required to secure optimal performance and a balance between computational costs and fidelity.

Another compromise is also faced regarding the options of turbulence modelling schemes, which is to a lesser extent covered by existing CFD guidelines. Direct Numerical Simulation (DNS) can accurately replicate turbulent flows, but this requires solving the Navier-Stokes equations at the Kolmogorov micro-scale, which is extremely demanding and makes DNS inaccessible to most CFD users. As a result, assumption-based turbulence modelling is commonly used. Such assumptions have categorised corresponding turbulence modelling strategies into several groups, known as Reynolds-Average Navier-Stokes equations (RANS), Large-Eddy Simulation (LES) and their combination (Hybrid). These schemes equip different capabilities, and one can require thousandfold computational resources than another (Tezdogan et al., 2015; Liefvendahl and Fureby, 2017). Therefore, it is of great importance to justify that an appropriate turbulence modelling scheme has been applied.

First of all, it is essential to use a turbulence modelling strategy when simulating ship flows, rather than just adopting a laminar assumption, because the kinematic energy dissipation within turbulent flows, if non-negligible, has to be taken into consideration. Khojasteh et al. (2020) compared shipping waters predicted by laminar modelling, turbulence modelling and experiments. They demonstrated that laminar modelling could cause a significant deviation in the fluid shape as well as the calculated velocity and force. They showed that such deviation could be avoided when applying RANS turbulence modelling. Moreover, researchers have proven that appropriately choosing a turbulence modelling strategy can provide accurate predictions in ship resistance (Zha et al., 2014a), motions (Cha and Wan, 2015) and wake (Shen et al.,

2002), as well as replicating complex ship flows such as propeller cavitation (Watanabe et al., 2003) and vortex shedding (Arslan et al., 2016). However, some turbulence schemes may cause important phenomena to be wholly neglected. For example, the time-averaging process of RANS negates the flow unsteadiness; thus, the cavitation observed in experiments could not be appropriately modelled when using RANS, as illustrated by Bensow (2011). Another example of Arslan et al. (2016) shows that small-scale fluid vortexes that are essential for predicting local structural response were captured by LES but not by RANS.

In such a context, appropriately choosing a turbulence modelling strategy becomes crucial when simulating ship hydrodynamic flows. Ideally, CFD users should count on a clear and up-to-date recommendation of suitable turbulence modelling schemes for different scenarios. The guidance is expected to avoid unnecessary testing time and improve simulation accuracy. To serve such a purpose, this work intends to provide a study on the applicability of available turbulence schemes while focusing on the applicability in model-scale and full-scale ship hydrodynamics. Being specific and critical, this work aims to provide handy insights on how existing turbulence modelling schemes can simulate ship hydrodynamic behaviours, focusing on their capability, limitation, computational cost and accuracy.

The present paper starts by briefly introducing the theories of different turbulence modelling schemes, linking to a review of how those schemes have been applied to various ship-flow interaction scenarios. Next, each scheme's capability and limitation are discussed and insightful explanations are given. Subsequently, turbulence modelling selection recommendations are provided based on a combination of well simulating the case and saving the computational cost, with respect to particular scenarios such as resistance prediction, ship flow modelling, self-propulsion, and cavitation. Finally, the paper discusses the main challenges faced by contemporary turbulence modelling methods and offers suggestions for future work.

2. Turbulence Modelling Approaches

2.1 Direct Numerical Simulation (DNS)

DNS principle is based on a direct resolution of the Navier-Stokes (N-S) equations representing the most complete mathematical description of the continuum flow of a fluid. Therefore, DNS is recognised to be the most expensive method to simulate turbulence flows. The N-S mass and continuum conservation equations are given below in the most general way (Peric and Ferziger, 2002).

$$\nabla \cdot \mathbf{v} = 0 \tag{1}$$

$$\frac{\partial(\rho \mathbf{v})}{\partial t} + \nabla \cdot (\rho \mathbf{v}\mathbf{v}) = -\nabla p + \nabla \cdot \tau + \rho g \tag{2}$$

where $\mathbf{v}$ is velocity vector, P is pressure, ρ is the density and $\boldsymbol{\tau} = \mu\left(\nabla \mathbf{v} + \nabla \mathbf{v}^{T}\right)$ is the viscous stress, in which μ is the dynamic viscosity.

Any DNS simulation requires to solve all essential scales of motion contained in the flow up to an order of magnitude of the Kolmogorov micro-scale (η_k) (Kolmogorov, 1941):

$$\eta_k = \left(\frac{\nu^3}{\varepsilon}\right)^{1/4} \tag{3}$$

where ε represents the dissipation rate and ν the molecular viscosity. In general, Kolmogorov micro-scales refer to the smallest turbulent vortex scales in a turbulent flow at which the viscosity dominates and the turbulent kinetic energy is dissipated into heat. DNS is the most accurate tool available for modelling viscous flow; however, the prohibitive computational cost of DNS has hindered it from solving most industrial problems.

2.2 Reynolds-Averaged Navier–Stokes (RANS)

The prohibitive cost of DNS motivated the development of more affordable numerical strategies to account for the turbulence effects. One of the most common methods is the Reynolds-Average Navier-Stokes equations (RANS), in which instantaneous turbulent velocity is decomposed into its time-averaged and fluctuating quantities, by modifying the N-S equations into:

$$\nabla \cdot \overline{\mathbf{v}} = 0 \tag{4}$$

$$\frac{\partial(\rho \overline{\mathbf{v}})}{\partial t} + \nabla \cdot (\rho \overline{\mathbf{v}\mathbf{v}}) = -\nabla \overline{p} + \nabla \cdot \left(\overline{\tau} - \rho \overline{\mathbf{v}'\mathbf{v}'}\right) + \rho \mathbf{g} \tag{5}$$

where $\overline{\mathbf{v}}$ is the time-averaged velocity and $\mathbf{v}'$ is the fluctuating one, ρ is the fluid density, $\overline{p}$ denotes the time-averaged pressure, $\overline{\tau} = \mu[\nabla v + (\nabla v)^T]$ is the viscous stress term, μ is the dynamic viscosity and $\boldsymbol{g}$ is the gravitational acceleration.

As additional unknowns have been introduced into equation (5), some approximations and additional models are required to solve the new appeared term. To model this term, two approaches are typically used:

a) Eddy viscosity models. This approach relates the turbulent stresses appearing in the RANS equations to the gradients of time-averaged velocity (Peric and Ferziger, 2002). Most eddy viscosity models are based on the Boussinesq approximation. This approach relates the Reynolds Stresses to the mean velocity gradients. The most known turbulent models in this group are the Spalart-Allmaras (SA), the $k-\varepsilon$ family and the $k-\omega$ family; they have several branches specialising in different problems and adopt specific empirical coefficients based on data fitting for a wide range of turbulent flows (McComb, 1990).
b) An alternative approach to solve the Reynolds stresses is by using Reynolds Stress Models (RSM). An RSM model directly calculates all the specific Reynolds stress tensor components by solving their governing transport equations together with an equation for the dissipation rate (Peric and Ferziger, 2002). This turbulence model can predict complex flows than eddy viscosity models because the transport equations for the Reynolds stresses naturally account for the effects of turbulence anisotropy and streamline curvature. However, it is essential to remember that this model belongs to the RANS category, averaging pressure and velocities, leading to inaccurate prediction of the unsteady vorticity fields.

2.3 Large Eddy Simulation (LES)

Kolmogorov (1941) proposed to describe the turbulent energy spectrum and its eddies into a range of scales. LES's principal idea is to reduce the computational cost of DNS by filtering the Navier–Stokes equations and modelling the smallest turbulent scales in the flow (Smagorinsky, 1963). LES's main principle is to approach the modelling of turbulence by considering that the large vortical structures created by the geometry contain most of the energy within the bulk flow. Thus, LES resolves turbulent structures in space everywhere in the flow domain down to a grid limit, while it uses a Sub-Grid Scale (SGS) model to simulate the effect of small eddies (smaller than filter size) on the mean flow.

The difference between DNS and LES approaches are summarised in Figure 1. DNS resolves all turbulent scales down to the Kolmogorov micro-scale from the N-S equations, whereas LES only resolves the largest turbulent scales in the flow.

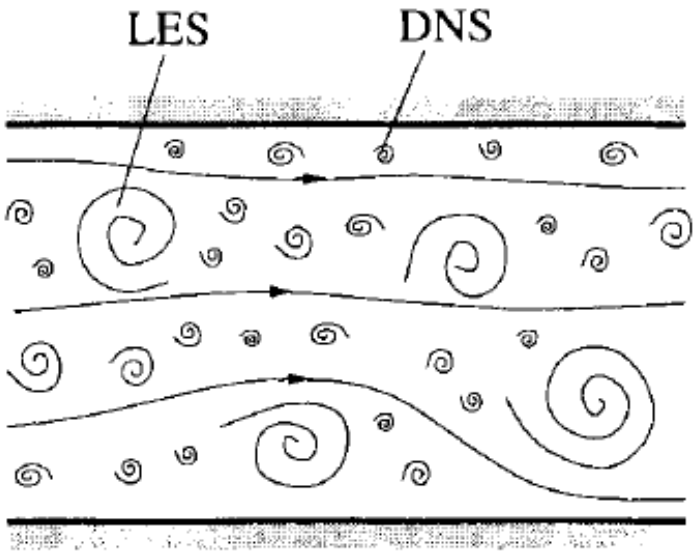

Figure 1: LES and DNS approach representation (Ferziger and Perić, 2002).

The low-pass filtering operation which is used in LES methods may be applied to spatial and temporal fields of a flow variable. In one-dimensional notation the filtered velocity (Leonard, 1975) is defined by:

$$\overline{u_i}(x) = \int G(x, x')u_i(x')dx' \tag{6}$$

where *G(x, x')* represents the filter kernel which has a length scale associated with it, Δ. Eddies with a size larger than Δ represent large eddies while those smaller than Δ represent eddies that need to be modelled. The Navier-Stokes equations can then be filtered to obtain the LES governing equations. More details can be found in (Ferziger and Perić, 2002).

For those scales smaller than the filter, RANS' Reynolds stress term in the governing equations is modelled using Sub-Grid Scale (SGS) models in LES. It is well known that in Newton's law of viscosity for incompressible flow:

$$\tau_{\text{Newtonian}} = 2\nu S = \nu\left(\nabla v + \nabla v^{T}\right) \tag{7}$$

where S is the rate of deformation of fluid elements. It has been found that the turbulent stresses increase as the mean rate of deformation increases. The Boussinesq hypothesis proposed that the Reynolds stress in RANS is proportional to the mean rates of deformation. In the SGS model, this theory is interpreted as SGS stresses are proportional to the instantaneous rates of deformation, i.e.

$$\tau = -2\nu_t S + \frac{1}{3}\mathrm{tr}(\tau)\mathbf{I} = -\nu_t\left(\nabla\overline{\mathbf{U}} + \nabla\overline{\mathbf{U}}^{T}\right) + \frac{1}{3}\mathrm{tr}(\tau)\mathbf{I} \tag{8}$$

where ν_t is the SGS eddy viscosity. On dimensional grounds, it is assumable that ν_t can be expressed as a product of an SGS velocity scale, ϑ, and an SGS length scale, L, as

$$\nu_t = C\vartheta L \tag{9}$$

where C is a dimensionless constant. Therefore, the turbulence model based on Eddy Viscosity theory is to find appropriate equations for ϑ and L by either algebraic relations or transport equations and then use them to obtain ν_t thus closing the filtered N-S equations; examples can be found in (Pope, 2001).

The main disadvantage of using pure LES for high Reynolds number flows is the requirement of very fine grids, particularly in the near-wall regions of the flow domain and very small time steps (Hanjalić and Launder, 2009). Therefore, it is anticipated that using LES for full-scale ship problems is not practical due to the high computational requirements.

2.4 Hybrid (RANS+LES)

Hybrid methods or RANS+LES methods are based on the principle of reproducing a RANS in regions not subjected to flow separation and an LES in regions with significant flow separation, respectively reflected as coarse and dense meshes, as presented by Guilmineau et al. (2018) in Figure 2. Hybrid methods were initially conceived for improving the numerical prediction of complex flows encountered in the aviation industry (Spalart et al., 1997). An example of this is the simulation of high–Reynolds flows subject to significant flow separation.

The concept of a hybrid method can be considered remarkably useful in ship hydrodynamics. For example, some problems require accurately modelling the ship's wake using a more detailed calculation of large eddy turbulent interactions, which can be done using LES. By contrast, regions of less complex physics can be calculated satisfactorily using RANS models. Such a hybrid approach is typically useful during propellers' design and performance evaluation and energy-saving devices or cavitation assessments.

Hybrid methods are typically classified into two categories: zonal and non-zonal methods. On the one hand, hybrid zonal methods rely on a RANS model and a subgrid-scale model. This approach is applied in different domains separated by a sharp or dynamic interface. By contrast, non-zonal methods assume that the governing set of equations smoothly converts from a RANS behaviour to an LES behaviour, based on criteria updated during the computation. Zonal hybrid methods have been successfully validated to resolve ship hydrodynamic problems, being Detached Eddy Simulation (DES) the most popular.

In general, DES is computationally cheaper than LES while able to simulate detailed turbulent vortex structures. Figure 3 shows the results from the flow's simulation at low Reynolds numbers for a sphere using different turbulence modelling strategies (Constantinescu et al., 2003). The figure reveals that RANS models cannot model the vortex shedding phenomena with details obtained during the LES and DES computations. In this case, all models were meshed using the same number of elements; however, DES was considerably faster than LES.

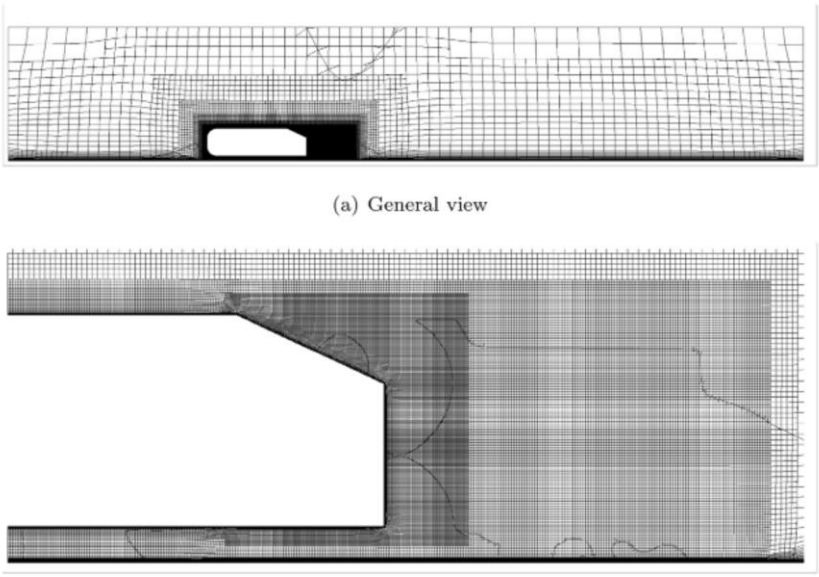

(a) General view

(b) Zoom at the back of the model

Figure 2: Hybrid mesh of Guilmineau et al. (2018): panel (a) shows general mesh in line with the requirement of RANS, panel (b) shows LES level mesh applied to the region where significant flow separation is expected.

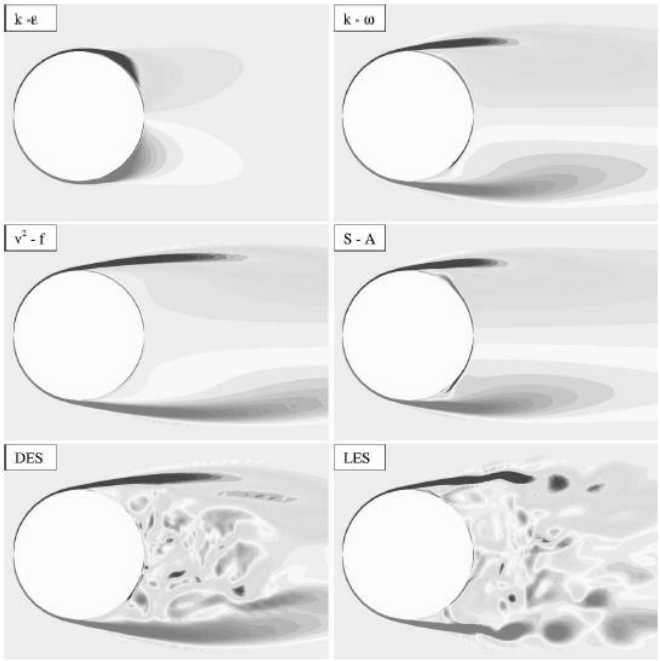

Figure 3: Turbulence modelling strategies comparison made by Constantinescu et al. (2003).

2.4.1 Detached Eddy Simulation (DES)

Compared with RANS and LES, DES is a new turbulence strategy that has been developed in recent years. DES allows the near-wall region to be treated by RANS, and regions of significant flow recirculation are modelled using an LES approach. The interface between RANS and LES is called the 'grey region'. The first DES (also known as the DES97) relied upon the isotropic Spalart-Allmaras (SA) model. The DES97 creates a hybrid method by introducing the cell size dependency into the SA turbulence modelling approach's destruction term. By these means, the detached eddies distant from the wall are resolved using LES, whereas the attached vortices are modelled using RANS. For this reason, the DES97 method was entitled the Detached-Eddy Simulation (Spalart et al., 1997).

The DES length scale was introduced to replace d_w in all terms of the SA model equations as follows:

$$L_{DES97} = \min(d_w;\ L_{LES}),\quad L_{LES} = C_{DES}\Delta,\quad \Delta = \max(\Delta_i, \Delta_j, \Delta_k) \tag{10}$$

Where $d_w < L_{LES}$, the DES length scale is equal to the RANS SA model length scale. By contrast, where $L_{LES} < d_w$, the length scale L_{LES} is employed. Being C_{DES} a constant and Δ corresponds to the grid size formulated as the maximum cell length in each index direction. This formulation is proposed assuming that no knowledge of the local turbulent structure is available in advance. The smallest resolvable isotropic eddies would scale with the coarsest grid cell dimension. Therefore, the DES97 formulation can successfully relate a near-wall region to RANS and fine mesh regions far from the wall to LES. However, this method reported several fundamental issues as follows.

The first issue is called 'The Grey Area'. The grey issue was known by Spalart (2009) and it refers to the zone where the DES model switches from RANS to LES mode ($d_w \approx C_{DES}\Delta$). This region was reported to be problematic unless the separation is abrupt and fixed by the geometry (Spalart, 2009). As the DES97 stipulates, the attached boundary layer should be handled entirely by RANS mode, where the turbulent kinetic energy is fully modelled. By contrast, the region containing flow separation should be handled by LES, fully resolving the turbulent kinetic energy. Therefore, a region between the two modes may contain little resolved turbulence even though the computation is in LES mode. The grey area issues are well known by DES users and tend to be more noticeable in flows with thin recirculation regions (Spalart, 2009). Also, problems can be encountered if the grid is too fine for the RANS region or too coarse for the LES region

247 which can lead to too little turbulence is modelled in the RANS region and too little turbulence is resolved
248 in the LES region, This phenomenon is called 'Modelled Stress Depletion' (MSD) (Spalart et al., 2006).

249 The second issue is called the 'Incursion of LES Mode Inside the Boundary Layer'. The DES97 was based
250 on the assumption that the near-wall tangential grid spacing exceeds the boundary layer thickness and only
251 outside the boundary layer limits d_w should be equal to $C_{DES}\,\Delta$. Nevertheless, the issues associated with this
252 condition's violation were anticipated in the original DES97 publication (Spalart, 2009). Menter and Kuntz
253 (2004) reported the former issue as part of their investigations using the DES97 model for an airfoil with
254 flow separation near the trailing edge. In general, their analysis predicted a separation point further upstream
255 than the location found by using a pure SA model. This phenomenon was named 'Grid Induced Separation'
256 (GIS). Overall, this issue affects the RANS Reynolds stresses that reduce the RANS mode's skin friction
257 calculation in certain situations. Therefore, the grid resolution's sensitivity that gives rise to the appearance
258 of MSD and GIS is identified as the most significant deficiencies of the original DES97.

259 The third issue is called the 'Log-layer Mismatch' (LLM). As reported by Nikitin et al. (2000), a consistent
260 pathology was found in DES where the modelled wall-shear stress deviates from the true one by
261 approximately 15%.

262

263 2.4.2 Delayed Detached Eddy Simulations (DDES) and Improved Delayed Detached Eddy Simulation
264 (IDDES)

265 The mathematical issues outlined in the previous section have been tackled by improvements in the original
266 DES97 turbulence modelling strategy. The most known improved versions of DES97 are the DDES and
267 the IDDES.

268 DDES can correct the MSD issue detected on the original DES97, which typically affects the RANS
269 Reynolds stresses calculations (Spalart et al., 2006). The DDES new capability detects boundary layers and
270 extends the RANS mode further, even if the cell size corresponds to an LES model. This model has also
271 demonstrated the ability to handle the GIS issue successfully. Hence, the method was proposed to replace
272 the DES97 even though it could not handle the log-layer mismatch yet. The IDDES is the latest and more
273 ambitious turbulence modelling strategy developed by Shur et al. (2008), which showed the potential to
274 solve the LLM in addition to the MSD issue. However, it is essential to emphasize that IDDES, is still
275 susceptible to mesh definition as much as DDES. An IDDES-based model may still present MSD if the
276 mesh is inappropriately defined.

A comparison between experiments and various turbulence modelling strategies is shown in Figure 4, where the vortex structure generated during the interaction of flow with a blunt body is presented. It can be seen that the IDDES method can accurately replicate the flow structure, while RANS approaches show a large deviation from the experimental observation.

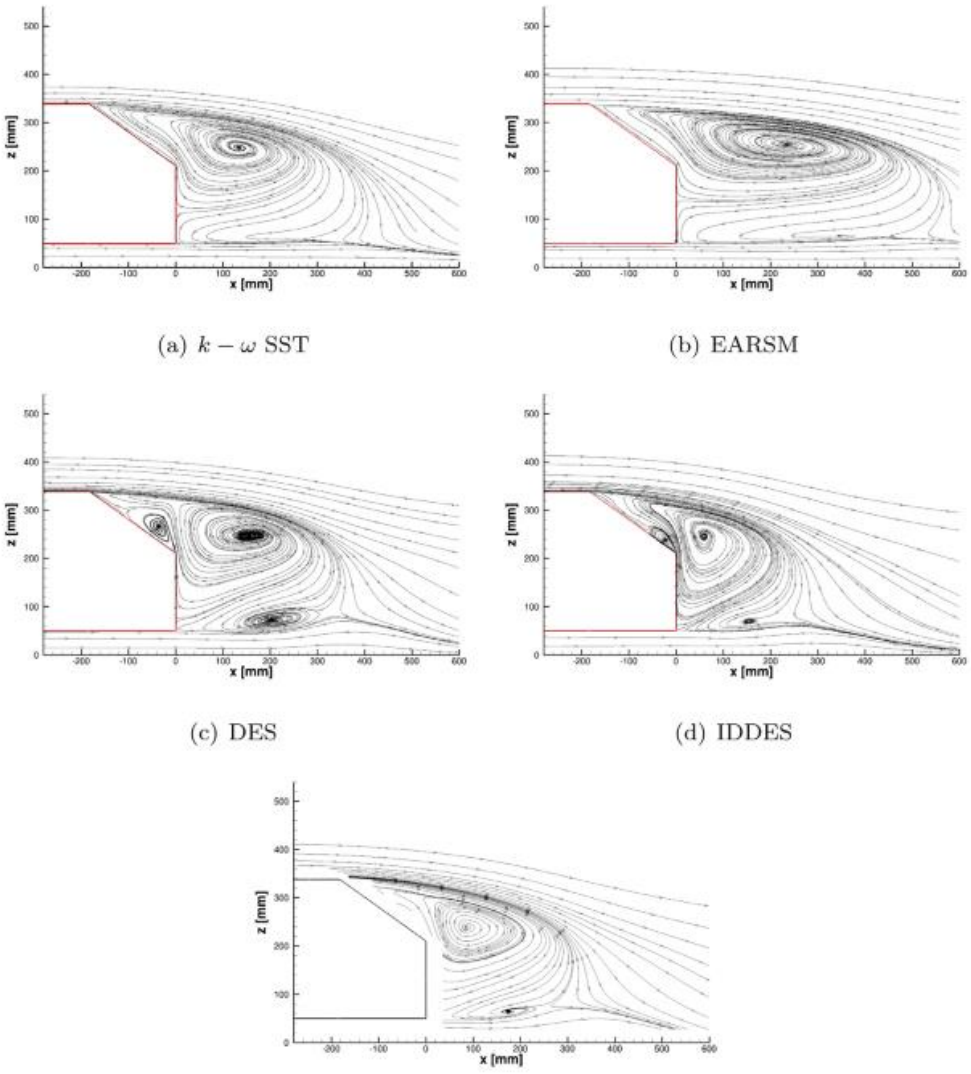

(a) $k-\omega$ SST (b) EARSM

(c) DES (d) IDDES

(e) Experiments

Figure 4: Flow behind a blunt body: a comparison between RANS (a) and (b), DES (c), IDDES (d) and experiments (e). (Guilmineau et al. 2018)

2.5. Turbulence modelling and y^+

The boundary layer of ships is commonly modelled by mesh layers built upon the hull surface in which the near-wall cell is very thin and the thickness of each contiguous layer gradually increases outwards so that the thickness of the outmost layer is close to the size of cells outside of the boundary layer mesh, as shown in Figure 5.

The y^+, as shown in Equation 11 (ITTC, 2014a), is the dimensionless quantity for the distance from the wall up to the centre of the first grid cell.

$$y^+ = \frac{h}{L_{pp}} \times Re\sqrt{0.0375/(\log_{10} Re - 2)^2} \tag{11}$$

where h is the thickness of the innermost cell layer, Lpp is the ship length between perpendiculars and Re is Reynolds number.

To calculate the near-hull fluid physics in CFD, y+ requires to be between 0 and 5 (most times y^+=1) which allows for the resolution of the boundary layer viscous sub-layer. This is translated in a very dense near-wall region which tends to result in computationally expensive simulations. On the other hand, Wall Functions (WF) can get around the unaffordable computational cost by modelling the inner part of the near-wall region (viscous and buffer sub-layers. When using WF, y+ tends to reach values significantly higher than 1 (in the order of 70-100 and even more). More details of WF can be seen in (Pope, 2001).

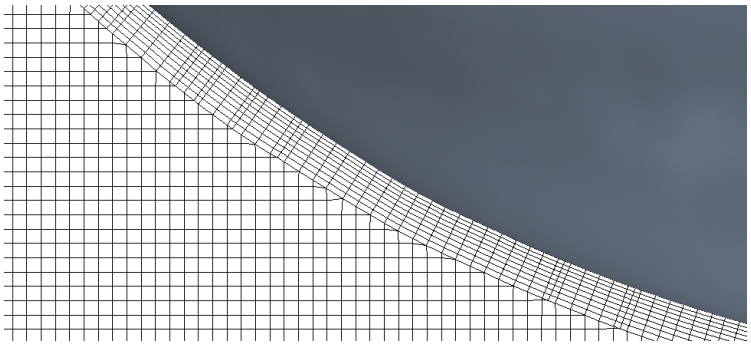

Figure 5: Illustration of near-hull mesh setup: mesh layers were built between the hull geometry (upper right) and uniform domain mesh (lower left).

In general, it has been well proved that RANS associated with WF allows accurate prediction of ship resistance when Y+ is up to 100, as also recommended by (ITTC, 2014a). However, except resistance prediction, a Y+ of 100 is not sufficiently accurate for other applications, such as propulsions ($y+ < 5$, (Sun et al., 2020)) and hydroacoustics ($y+ < 1$, (Smith and Ventikos, 2021)). Meanwhile, other turbulence schemes rather than RANS should be used in those applications, for which, a specific review will be given in Section 3.

3. Ship hydrodynamic applications

This section presents the state of the art of turbulence modelling strategies and their applicability for the prediction of ship resistance, boundary layer, propeller propulsion, cavitation, and structural vibration, alongside comments on their capability and limitations.

3.1 Resistance

DNS**,** the most complex and detailed strategy for modelling the flow, has been successfully applied to simulate free-surface turbulent wake behind ships in model scale (Shen et al., 2002). The authors tested three 50-cm towed ships with different beams to draft rations during the experiments and at very low Froude number Fr = 0.04. The hull forms were relatively simple, resembling a cylindrical shape as the main interest was to understand the underlying physics of turbulent wake at a Kolmogorov micro-scale and their dependence on basic hull geometric parameters. In general, the results from the DNS simulations (Figure 6) are satisfactorily comparative to the experimental results. However, it should be emphasised that the simulations were conducted at very low Reynolds numbers, far from real towing tank experiments.

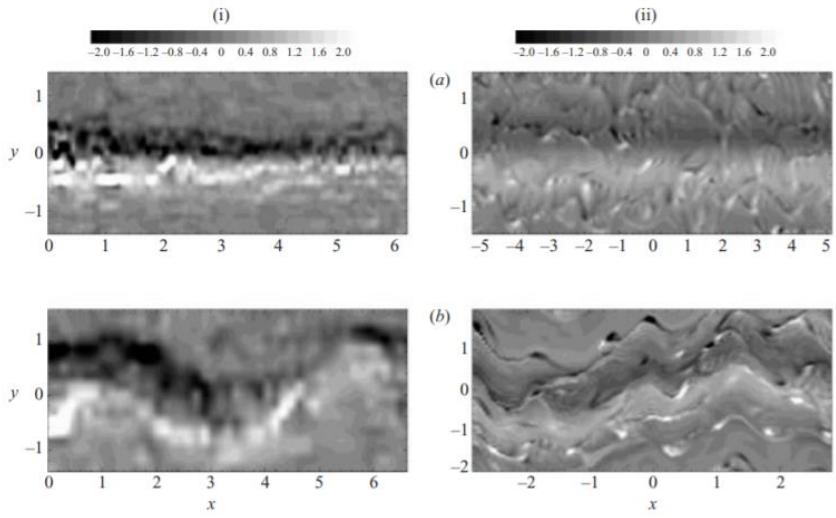

Figure 6: Instantaneous contours of spanwise vorticity ω_z of ship wake at the free surface, obtained using (i) experimental PIV technique and (ii) the DNS simulations. The upper and lower panels show two different hull geometries. (Shen et al., 2002)

DNS simulations for a realistic hull form geometry in full/model scale have not been reported yet. In general, simulations with much higher Reynolds numbers would present a significantly more turbulent flow. As a consequence, the Kolmogorov micro-scale η_k would reduce dramatically. For example, considering a full-scale DNS simulation of a typical cargo ship with a length L = 150 m at a Reynolds number $Re = 10^9$, for such a problem, it is expected that the Kolmogorov micro-scale will be in the order of at least 2×10^{-19} m. Therefore, modelling all the turbulent scales up to the Kolmogorov micro-scale would require an incredibly dense mesh with cell sizes in the ship wall's vicinity measuring at least 2×10^{-19} m. This numerical order of magnitude clearly shows that DNS implies a huge numerical task and remains unlikely to achieve in practice.

RANS has been successfully applied to predict ship resistance and the results agree well with test data (ITTC, 2017). Remarkable examples are validations against the model-scale KRISO Container Ship (KCS), designed by the Maritime and Ocean Engineering Research Institute of South Korea, the model-scale Japan Bulk Carrier (JBC), designed by the National Maritime Research Institute, Yokohama National University and Ship Building Research Centre of Japan, and the full-scale Ragel, a real general cargo ship. In addition, there have been a range of workshops reporting work on representative tests and comparing numerical approaches from different participants during blind tests which were validated with experimental data. Some examples are the Gothenburg (Larsson et al., 2013) and the 2015 Tokyo (Larsson et al., 2015)

workshops in ship hydrodynamics. These efforts have facilitated best practices of ship simulations that provide insights into the applicabilities of different numerical strategies (Eça et al., 2009).

According to the ITTC recommendation for resistance predictions (ITTC, 2014b), a y^+ value of 30~100 is in most cases sufficient when employing WF RANS. This conclusion was given as part of the 2015 Tokyo Workshop in Ship Hydrodynamics (Hino et al., 2020), where participants demonstrated that WF could achieve more accurate resistance prediction than directly resolving the wall region. Therefore, it is seen that WF is computationally cheaper than wall-resolved methods while it can still provide comparable resistance prediction. This phenomenon is related to the fact that ship resistance is an integral force value, not because WF obtained better fluid details than wall-resolved methods.

The computational cost of WF RANS is mostly affordable for standard computers nowadays. The ITTC suggested a value of y^+ 30~100 which needs several million elements of mesh for a full-scale container ship (Tezdogan et al., 2015, 2016), and the required elements will be much fewer for model-scale; Terziev et al. (2019) conducted comprehensive model scale resistance computations on the KCS geometry and demonstrated that RANS models could accurately obtain ship resistance when the total cell number is 1~3 million.

RANS eddy-viscosity models: SST $k-\omega$ and k-ε are the most common turbulence modelling strategies used to simulate viscous marine flows (Terziev et al., 2019). In terms of the numerical setup, RANS eddy-viscosity models shelter the mesh near ship walls from the extreme density of the Kolmogorov micro-scale. In general, the SST $k-\omega$ has been demonstrated to be a robust turbulence modelling strategy due to its capability to model adverse pressure gradients and flow separation (Paterson et al., 2003). A negative pressure gradient means the static pressure increases in the flow direction, which can happen when a water flow encounters a hull, especially around the stern region (ITTC, 2014b).

Model scale investigations using RANS have reached a certain maturity and confidence (Wackers et al., 2011). Abundant comparisons between RANS-CFD and model-test results reported good agreement, during open-water resistance, propulsion, seakeeping, and manoeuvring simulations. Zha et al. (2014a) demonstrated the SST $k-\omega$ model can be applied to accurately predict the resistance of large container/tanker ships and Zha et al. (2014b) shown that the same approach also works well for high-speed hulls. Yet, accurate results could also be obtained by the $k-\varepsilon$ method, as proved by Dashtimanesh et al. (2020).

Wackers et al. (2011) presented that the wake of an advancing ship can be modelled in a high-fidelity manner; Figure 7 and Figure 8 respectively show the validation of overall wave pattern and free-surface

line along the hull. The authors demonstrated that the selection of various RANS models does not make a significant difference in this particular application. Since ships' wave pattern is more of a qualitative criterion and subject to certain uncertainties, subtle disagreements between different RANS models are reasonable. Shen and Wan (2013) presented comparisons between RANS (the SST k-ω) simulations and the experiment of a ship advancing in head waves, demonstrating good accuracy for the prediction of ship motions and added resistance. The SST k-ω method has also successfully replicated measurements during CFD self- propulsion tests (Winden et al., 2014) and ship performance in confined waterways (Huang et al., 2020, 2021a, 2021b). In addition, Huang et al. (2021c) successfully reproduced the fierce water-entering process of a freefall lifeboat by the SST k-ω model, demonstrating that the calculated impact forces agree well with full-scale measurements. These examples clearly show that RANS models, particularly the SST k-ω model, can provide accurate predictions of ship resistance, motions and wave patterns.

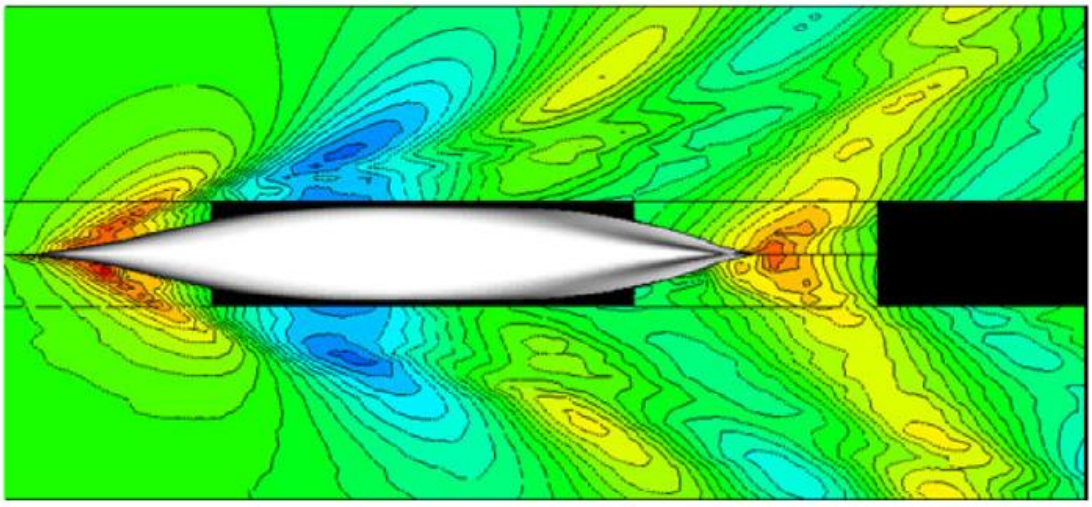

Figure 7: Comparison of computed (top) and measured (bottom) wave pattern for the Series 60 ship (Wackers et al., 2011).

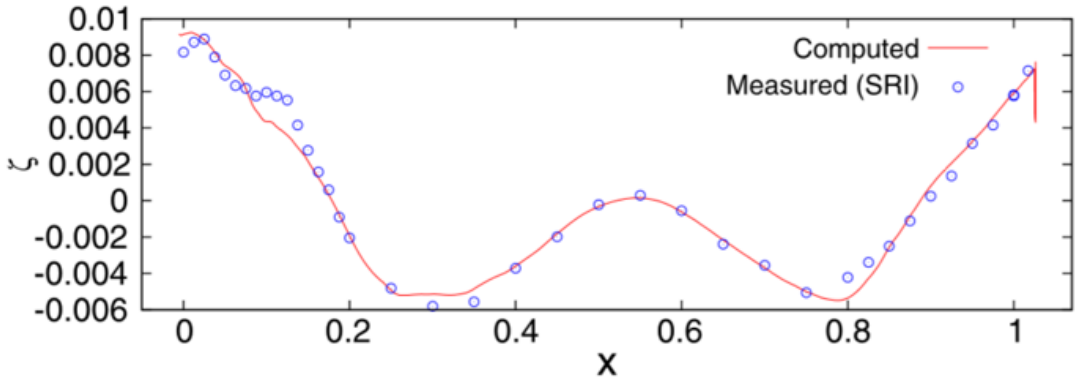

Figure 8: Validation of wave profile for the standard Wigley hull advancing in calm water. (Wackers et al., 2011)

In shallow water CFD simulations, Terziev et al. (2019) compared results from different eddy viscosity models with experimental results to calculate ship resistance. They demonstrated that the results from different RANS schemes are at the same accuracy level, as shown in Figure 9.

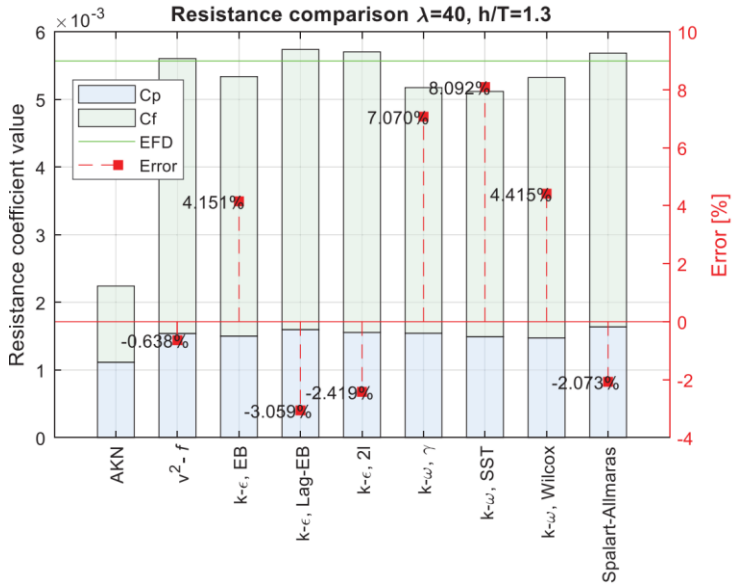

Figure 9: Resistance deviation of different RANS eddy viscosity models. (Terziev et al., 2019)

In full scale, turbulence modelling strategies validations for the simulation of ship viscous flows have barely been conducted. In general, it is known that Reynolds number differences between full-scale and model-scale simulations significantly affect the boundary layer structure. This leads to considerable discrepancies between ship hydrodynamics in model scale and full scale. ITTC provided a guideline on correlating ship resistance from model-scale to full-scale by correcting the viscous resistance (ITTC, 2008). However, detailed physical features would not be able to be revealed using such a correlation approach. It is worthy to mention that the hull roughness is particularly influential for full-scale modelling, because higher skin friction results in a higher roughness Reynolds number, which makes the scale effect significant. The validation study of Song et al. (2021) shows different levels of roughness setups in CFD will result in different boundary layer behaviours as well as resistance deviations against experiments, where the modelling of roughness in CFD is achieved by modifying the WF model. The detailed equations for roughness modelling can be referred to (Song et al., 2021).

Unsteady flow features have been successfully modelled by using the Reynolds Stress Model (RSM). Sotiropoulos and Patel (1995) compared the stern and wake flow predicted by an eddy viscosity model and RSM. The comparisons show that the RSM accurately predicts most of the experimentally observed flow features in the stern and near-wake regions, whereas the two-equation model predicts only the overall qualitative trends. In particular, solutions with the RSM accurately display the origin of the stern vortex. Furthermore, Zou et al. (2010) shown the excellent capability of an EARSM model (Explicit Algebraic Reynolds Stress Model) (Deng et al., 2005) on simulating manoeuvring, by which they presented a tanker performing turns at different speeds; and Mucha et al. (2016) reported that both the EARSM and the SST k-ω RANS models can accurately predict ship hydrodynamics in a canal scenario. Although RSM has shown the potential of obtaining better accuracies than eddy-viscosity based RANS models on flow feature predictions, it has a much higher computational requirement. Thus, RSM usage has not been popular in ship design, since the much cheaper eddy-viscosity-based RANS can already offer a relatively accurate prediction on the integral performance of ships, e.g. resistance or motions.

IDDES ship resistance calculations found in the literature were performed by Kornev et al. in model scale (2011). The authors compared the ship resistance components' prediction using an IDDES based computational model vs different RANS turbulence approaches. Their investigation showed that the IDDES set-up could predict the total resistance with just a 1% deviation from the experimental results measured during the towing tank calculation (Kornev et al., 2011). By contrast, all RANS models deviated from the experimental outputs with a margin between 3% to 7.5%.

Another set of model scale ship resistance calculations using the IDDES formulation with a y^+ of less than one were performed by Kornev et al. (2018). This time, they tested the Japan Bulk Carrier (JBC) benchmark test case presented during the 2015 Tokyo workshop in Ship Hydrodynamics (Hino et al., 2020). They compared the ship resistance components' prediction when using an IDDES based computational model vs RANS calculations. Their investigation showed that the IDDES set-up could predict the total resistance with a 4% deviation from the experimental results measured during the towing tank calculation (Kornev and Abbas, 2018). The RANS set-up, however, deviated by just 2.3% from the experiments.

In addition, Kornev et al. (2018) compared RANS and IDDES on predicting friction and pressure resistance components, C_F and C_P, and the results were unexpected. The RANS setup C_F was compared with calculated C_F using the well-known ITTC-57 friction line (ITTC, 1957), showing a 2% deviation between the CFD output and the empirical friction line. By contrast, the IDDES computational setup deviated by 15% from the ITTC57 empirical formulation. Kornev et al. (2019) attributed this deviation to the difficulty to reproduce the turbulence transport through the interface between the RANS and LES zones. They believe that the LES area approaches the wall on certain occasions, resulting in an underestimation of the vortex generation in the near-wall region. This phenomenon results in a Grid Induced Septation, which overpredicts the pressure resistance. Nevertheless, the ITTC friction line was designed for ship hull geometries built before 1957. Therefore, considering the demonstrated accuracy of the IDDES for calculating the total resistance, a deviation in C_F with the 1957 experimental line could be impractical when analysing a modern hull form.

Kornev et al. (2018) results may not be taken as conclusive. It has been observed that the RANS setup showed grid convergence between the mesh refinements. However, for the IDDES case, it can be seen that setup convergence was not fully achieved, and perhaps one further refinement would have been needed. Moreover, RANS simulations demonstrated to provide substantially accurate results when compared to sea trials. Therefore, it seems that there is not much room for further improvement by IDDES.

LES for ship resistance modelling has been shown to be prohibitive as well as unnecessary. Liefvendahl and Fureby (2017) estimated the cell number of LES required to simulate a whole hull are around 8×10^8 in model-scale and around 6.7×10^{13} in full-scale. Simulations may be therefore achievable in model-scale (Nishikawa et al., 2012) but still unaffordable in full-scale even though High-Performance Computing (HPC) facilities are available. To date, there is no publication found on simulating a whole full-scale ship using LES, partially because it is too expensive, and also because RANS has been widely proved accurate enough to provide an estimation of integral forces such as resistance or thrust.

3.2 Boundary layer and propeller wake

Boundary layer (local flow) and wake studies tend to be significantly more complex than resistance investigations. The Tokyo 2015 Workshop in Ship Hydrodynamics (Larsson et al., 2015) closely examined the accuracy of different turbulence modelling strategies and different wall treatments for different geometries. When applying RANS turbulence approaches to high block coefficient ships such as the JBC in model scale, where significant flow separation is expected, it was found that using low values of y+ provides a more accurate boundary layer structure than high y+. This is displayed in Figure 10, which compares experimental measurements of the non-dimensional velocity (left subfigure) against CFD computations using wall modelled RANS (high y+, middle subfigure) and wall-resolved RANS (low y+, right subfigure). The comparison shows that only low y+ functions were able to calculate the 0.4 non-dimensional velocity isolines. Based on the comparison wall-resolved RANS performs better than wall-modelled RANS when flow separation is important.

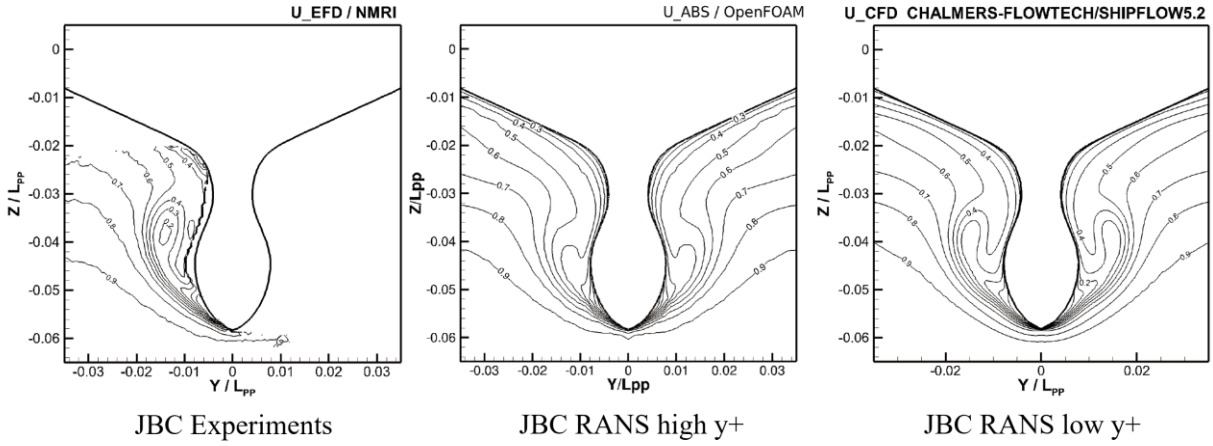

Figure 10: Velocity contour comparison for the model-scale JBC geometry between experiments (left), high y+ (middle) and low y+ (right). (Larsson et al., 2015)

Kornev et al. (2018), who participated in the 2015 Tokyo Workshop, studied the velocity contours on the aft region for the JBC hull with a high block coefficient ($C_b > 0.8$) in model scale. The authors compared a RANS and an IDDES with experimental results at a Re = 7.46 x 10^6 as shown in Figure 11. The figure shows the results from the towing tank tests, the IDDES approach's results, and the computations using the RANS SST k-ω. In general, it can be seen that the IDDES approach was able to capture the bilge vortex

with a high degree of precision. Therefore, the experiments corroborated the enhanced IDDES' capability to accurately predict the vorticity and vortex shedding structures emanated from the hull. The authors also remarked that IDDES capability is particularly noticeable if $C_b > 0.8$. By contrast, the RANS model significantly deviated from the experimental results and calculated a much weaker bilge vortex, which indicates that the unsteady turbulent behaviours can be eliminated by the averaging-process of RANS, alongside corresponding structural vibrations.

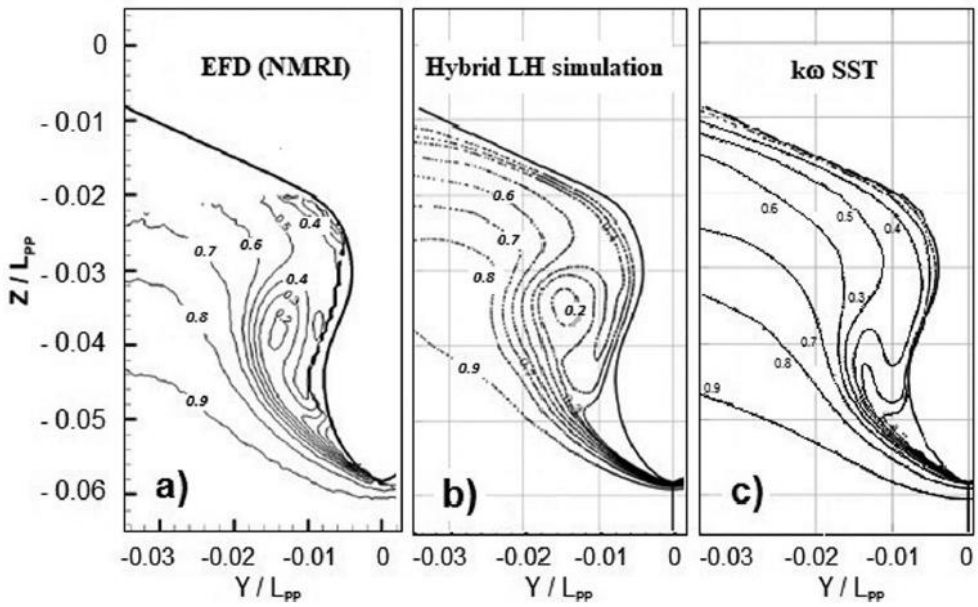

Figure 11: Study of the instantaneous velocity contours on the aft end of a model scale ship by (a) model scale experiments, (b) IDDES and (c) RANS. (Kornev et al, 2018)

DES models are known to overperform RANS when separated flows are expected. A typical case is seen when computing geometries both slender and bluff bodies at a static drift angle (Xing et al., 2012) and (Bhushan et al., 2011). However, for low-blocky ships with minimal separated flows, the literature reveals some limitations in DES models. For example, the 2010 Gothenburg Workshop in Ship Hydrodynamics (Larsson et al., 2013) reported that DES models suffer from modelling issues such as Modelled Stress Depletion (MSD) which manifest as a difficulty to reproduce the turbulence through the interface between RANS and LES zones in the flow attached regions (Spalart et al., 1997). MSD is seen in cases when the LES length scale drops below the RANS length scale close to the wall region, triggering the numerical model into LES mode close to the wall. In such a scenario it is possible that the desired LES region is not

refined enough and cause an error. This issue may significantly affect the performance of the model for non-separated flows, which are more typical on low block coefficient geometries. As corroboration of this theory the 2010 Gothenburg Workshop (Larsson et al., 2013) and 2015 Tokyo Workshop (Hino et al., 2020) both confirmed that RANS models are able to provide a good representation of the wake and accurate self-propulsion results for low blocky ships, such as KCS and DTC.

Viitanen et al. (2018) conducted open water model scale marine propeller DDES simulations that were compared with experimental results. Propeller global forces, local flow phenomena, and cavitation patterns were compared to cavitation tunnel tests results. As shown in Figure 12, the results from their investigation suggested that the DDES numerical approach accurately predicted the flow pattern. The authors emphasised that the propeller's DDES open water characteristics underpredicted the thrust by 2-8%. By contrast, the torque was accurately predicted with minimal deviations of just 1%. The author attributed the deviations to possible confinement effects due to the geometry of the cavitation tunnel, which was simplified during the simulations. This study also found a good agreement between the numerically simulated propeller wake patterns and experimental LDV measurements.

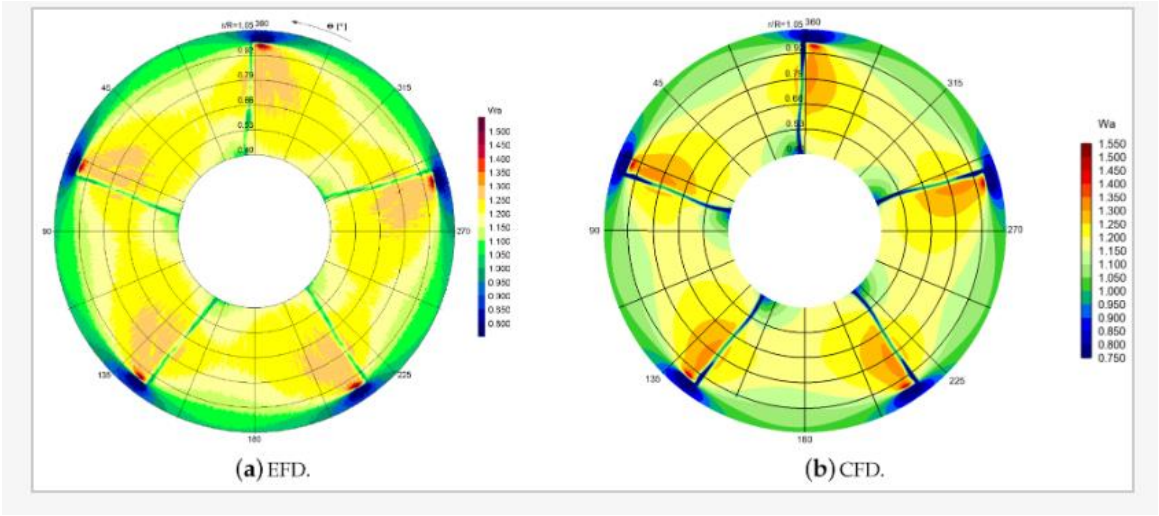

Figure 12: Effective wake for open water marine propeller (a) experimental results and (b) DDES (Viitanen et al., 2018)

The enhanced capability of the IDDES has also been noted in full-scale. Pena et al. (2020a; 2020b) compared nominal wakes (Figure 13) and vorticity fields on the aft end of the ship in full-scale. Two RANS turbulence modelling approaches suitable for the simulation of ship flows have also been assessed: the k-ε

model and the k-ω SST model. The results from their investigations revealed significant deviations from the calculation of the wakes in full-scale when using different turbulence modelling strategies. Both RANS setups demonstrated a fair agreement. Differences were observed in the region closer to the propeller centre. More substantial velocity retardation and a higher degree of three-dimension of the wakefield can be seen for the SST model. On the other hand, the hybrid IDDES model showed close to zero velocity fluid on the region under the shaft.

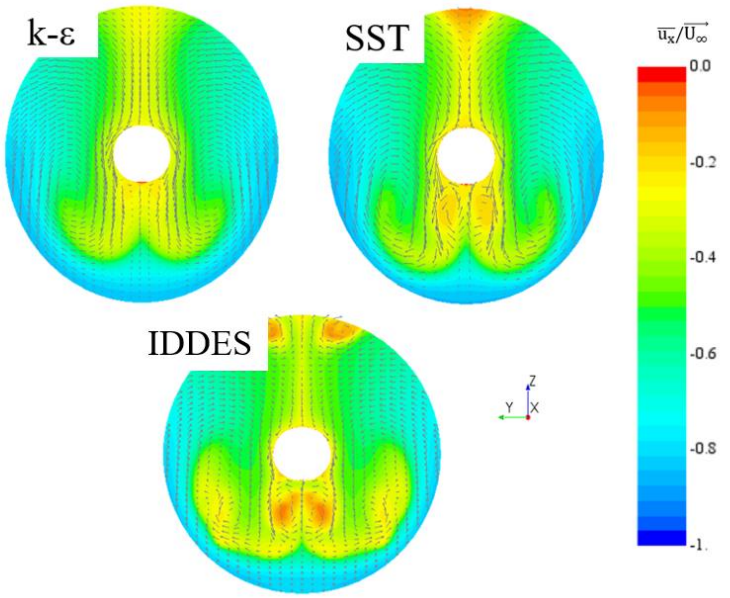

Figure 13: Nominal wake prediction using different turbulence modelling strategies Pena et al. (2020a; 2020b)

The work of Pena et al. (2020a; 2020b) confirmed that RANS numerical simulations in full scale resulted in a less accurate prediction of the velocity fields within the ship boundary layer and wake. For the first time, they attributed numerical issues linked to choosing an improper turbulence modelling strategy to the discrepancies between sea trials and numerical simulations of energy-saving devices performance (ITTC, 2014b). They recommended using an IDDES-based numerical approach to investigate the wake and boundary layer of full-scale ships with a particular focus on the design of propellers, rudders or energy-saving devices.

LES has been applied to predict high-vortex flows generated with a ship. Yang et al. (2008) simulated a whole ship in model scale using Wall Resolved LES (WRLES), as shown in Figure 14. Their results did

show that WRLES produced high-fidelity boundary layer structures, as shown in Figure 15. However, they reported that the simulations required a cell number of around 268 million even in model scale, which is hardly affordable in the industry. On the other hand, Liefvendahl and Fureby (2017) conducted model scale simulations of the JBC using Wall Modelled LES (WMLES) and WRLES approaches in model scale with meshes of 19 million and 800 million elements respectively. From Liefvendahl et al. experience, it is possible to remark that the WRLES approach is feasible if only one simulation is required, while ship design usually needs to run extensive simulations considering a combination of different inputs (e.g. operation condition, ship hull variant). A later study from Liefvendahl and Johansson (2021) compared again the two approaches and its applicability in the marine industry for the prediction of model scale ship bulk carrier. Their investigation showed that WMLES is feasible for model scale ship hydrodynamics and with substantial mesh savings when compared to wall-resolving LES. Therefore, WMLES could be the solution to make LES accessible for full ship simulation.

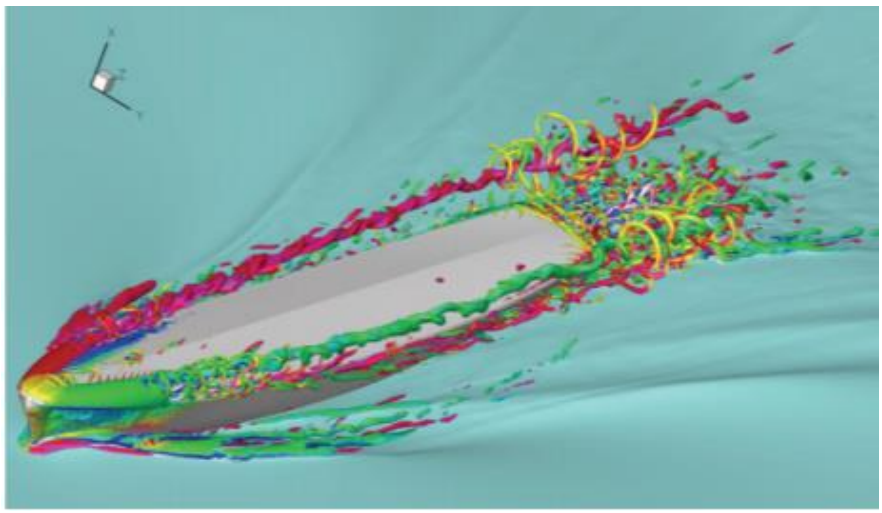

Figure 14: LES simulation of vortex structures associated with an advancing ship. (Yang et al., 2008)

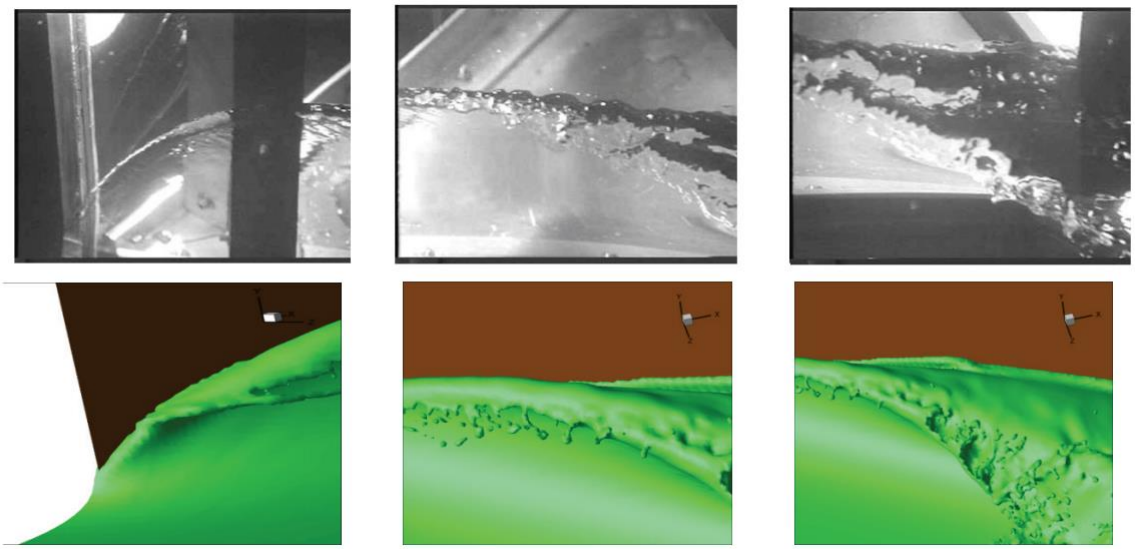

Figure 15: Flow pattern comparison near the bow. (Yang et al., 2008)

Alternatively, LES can be applied to localised ship design. In this manner, high-density meshes are just needed to be applied to a part of a hull where turbulent behaviours are of great significance. For example, Arslan et al. (2016) put only two-dimensional sections of a hull into LES simulations, thus investigating the motions of a ship subjected to lateral flows, i.e. cross currents. They provided parallel CFD and model-test comparisons to show that considerable vortex structures are generated near the ship section and can bring about instability to manoeuvring, with LES's excellent capability illustrated by Figure 16. Moreover, they reported RANS failed in this case, as the small-scale vortexes are roughly left out and the vortex centre is inaccurately predicted, see Figure 17. Thus, it remains doubtful on applying RANS to predict the vortex structures associated with the interactions of flow with a certain ship part. More examples of comparing LES and RANS in localised ship design will be presented in Section 3.4.

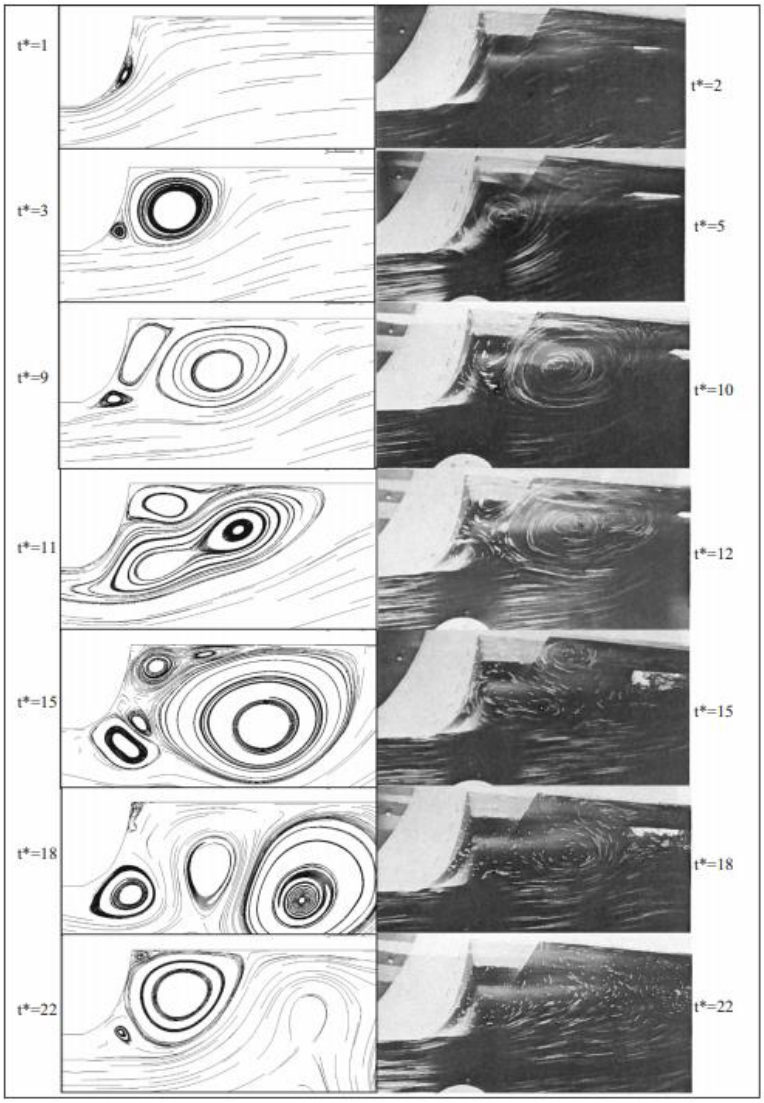

588

589 Figure 16: LES (left) and experimental (right) views of vortex structures occurring when a lateral section
590 of a hull is subjected to a cross current. (Arslan et al., 2016)

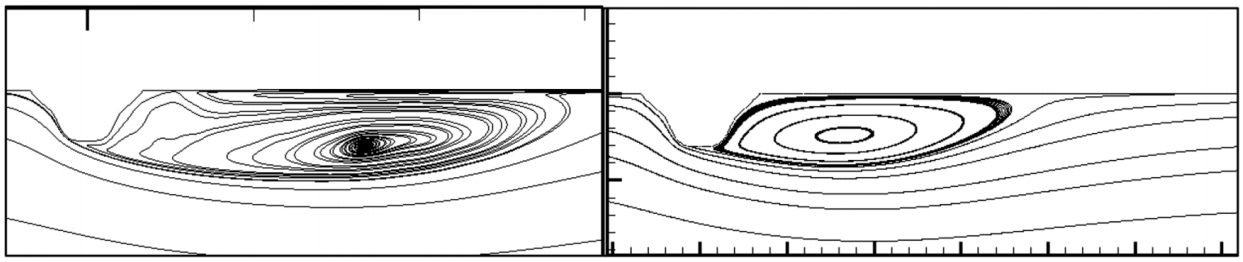

591

592 Figure 17: LES (left) and RANS (right) views of vortex structures occurring when a lateral section of a
593 hull is subjected to a cross current. (Arslan et al., 2016)

3.3 Self-Propulsion

Self-propulsion simulations in full scale revealed that RANS could provide accurate propeller thrust and torque predictions using the sliding mesh approach (Ponkratov and Zegos, 2015; Pena et al., 2019), or the actuator disc approach (Jasak et al., 2019; Bakica et al., 2020). Both approaches have demonstrated provide results in line with the Lloyds Register First Full-scale Ship Hydrodynamics Workshop (Lloyds Register, 2016). Jasak et al. (2019) demonstrated that using the SST $k-\omega$ RANS scheme could achieve agreement with experiments with only 6 million cells, as shown in Figure 18, while it should be noted that Jasak et al. did not discretise the propeller geometry which results in less computational mesh requirements. It should also be noted that they used very sophisticated local mesh refinements in their in-house code, shown in Figure 19, which may be hard to replicate by others. This indicates local mesh refinements can be an important skill when considering the compromise between turbulence modelling strategies and computational costs. Nevertheless, the results are still encouraging as even 10~20 million cells would be affordable with HPC that have been popularised nowadays.

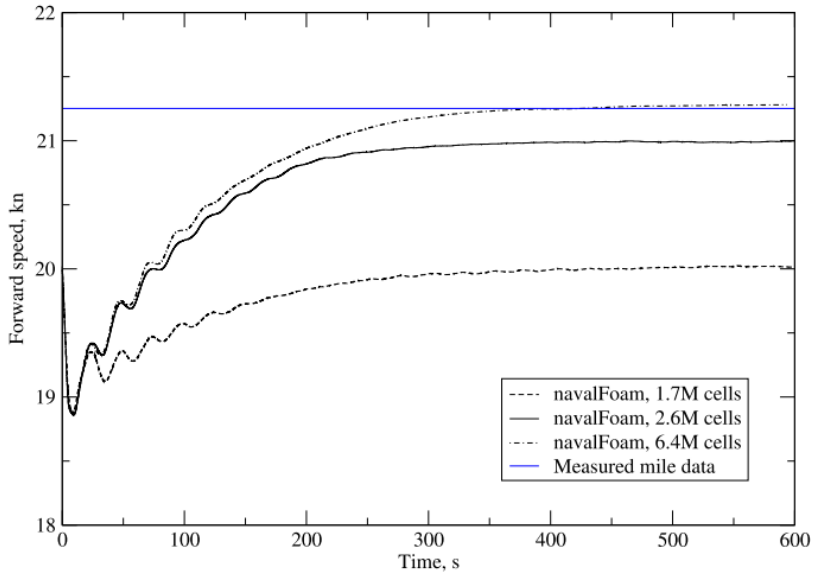

Figure 18: Mesh sensitivity study for predicting self-propulsion thrust, alongside a comparison with full-scale measurement data. (Jasak et al., 2019)

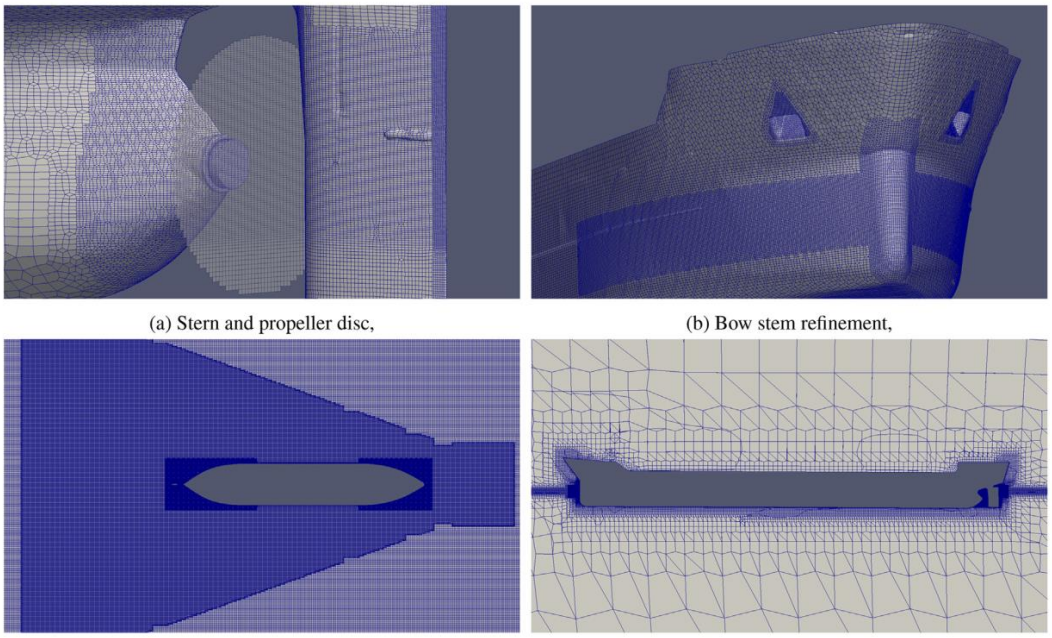

(a) Stern and propeller disc, (b) Bow stem refinement,

(c) Kelvin angle refinement, (d) Free surface and near hull refinement.

612

613 Figure 19: Mesh layout of a self-propulsion ship in full scale, in which sophisticated local mesh
614 refinements are applied. (Jasak et al., 2019)

615

616 Using DES, model scale self-propulsion simulations in rough waters were conducted by Carrica et al.
617 (2011) based on a fully discretised propeller with dynamic overset grids approach. They compared results
618 between CFD computations and experiments and showed deviations in calculating the thrust and torque
619 coefficients K_T and K_Q of 6% and 5%, respectively. The deviances with the experimental results are likely
620 to be minimised by implementing an IDDES numerical model to avoid the DES97 numerical issues.

621 Using IDDES, Kornev et al. (2018) numerically and experimentally compared model-scale calm water self-
622 propulsion tests using the JBC benchmark test case presented during the 2015 Tokyo workshop in Ship
623 Hydrodynamics (Hino et al., 2020). During the analysis the authors used the Arbitrary Mesh Interface
624 (AMI) module provided in OpenFOAM to model the interface between static (hull) and rotating (propeller)
625 grids with a y^+ of 2.9 at the propeller and 15 on the hull. As a result, the authors used dense meshes
626 exceeding 10 million elements, which requires high computational resources. The results from this
627 investigation revealed that K_T and K_Q were predicted with a degree of accuracy of 7% and 2% respectively.
628 They also used RANS to do the same validation exercise and found that the RANS set-up showed a higher
629 degree of accuracy with K_T and K_Q deviances of 1 and 5% respectively.

Pena et al. (2020a; 2020b) compared the torque coefficients obtained at the self-propulsion point, using three different turbulence approaches, against the experimental values measured on the sea trials (Figure 20). This work was based on a ship geometry with a $C_b = 0.77$ and sea trial measurements that enabled the numerical model's validation. The authors remarked that three numerical models produced consistent results compared with the experimental data, with an 8% difference for the k-ε and a 5% difference for the SST. The IDDES was the most accurate of the three set-ups, producing results within an excellent 2% difference from the sea trials measurements.

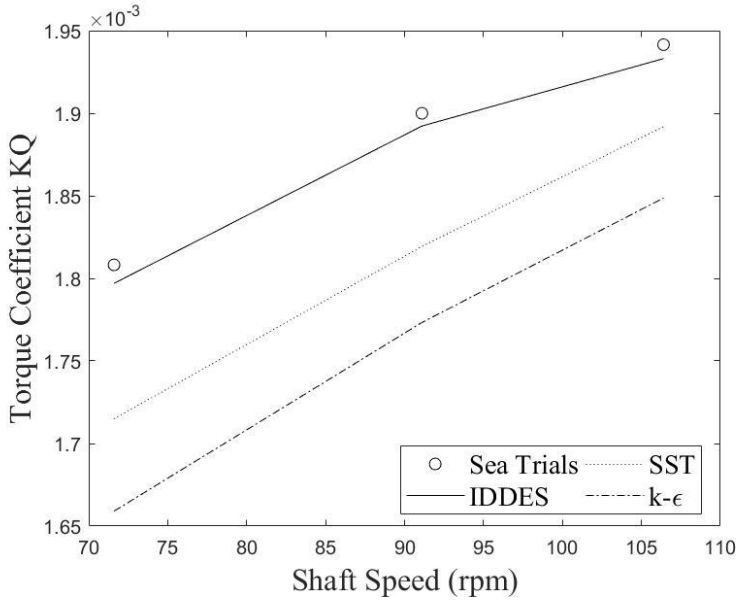

Figure 20: K_Q for the three turbulence modelling strategies and the experimental measurements at three shaft speeds. (Pena et al., 2020a; 2020b)

Also, a recent trend for self-propulsion modelling recommends the implementation of wall-roughness functions which seem to yield more accurate results than the ones obtained when using a smooth wall non-slip condition (Mikkelsen and Walther, 2020) and which may account for biofouling, the paint roughness, welding seams or hull plate deformations on the hull (Pena et al., 2020b). Implementing roughness in WF is expected to increase the boundary layer thickness and nominal wake disturbances as shown by Song et al. (2019), which may impact the calculated propeller performance. This new approach seems promising, however, multiple studies presented in the literature have shown accuracy during self-propulsion tests without the necessity of the implementation of wall-roughness in full-scale (Ponkratov and Zegos, 2015;

Ponkratov, 2017; Jasak et al., 2019; Pena et al., 2020b; Bakica et al., 2020). Therefore, further investigations are required to clarify the role of wall roughness for self-propulsion modelling.

The reviewed literature shows that it is not yet well-established which turbulence modelling strategy yields the most accurate results versus which propeller modelling approach (e.g. a virtual disk or a physical disk). Different approaches do not show an obvious difference in terms of macro-parameters calculation such as torque and thrust coefficients. For example, Carrica et al., (2011) using a physical-disk + DES approach obtained a higher level of K_T and K_Q than those obtained by Jasak et al. (2019) using a virtual-disk + RANS. It is therefore suggested to use a virtual disk approach to predict macro-parameters due to its relatively low computational requirements. By contrast, if local flows need to be studied as part of the self-propulsion analysis, then a fully discretised propeller approach is recommended. In this case, high computational resources (very dense meshes) will be required. If during the self-propulsion tests flow separation is expected and the unsteady loads at the propeller need to be studied, then may be recommended to implement a DES approach. However, the simplest cases with no flow separation could still be modelled by a RANS approach.

3.4 Cavitation

Cavitation is a phenomenon in which rapid changes of pressure in a liquid lead to the formation of small vapour-filled cavities in places where the pressure is relatively low, commonly occurring with the operation of propeller and hydrofoil. RANS has shown capable of generating gas-phase out of water-phase during propeller cavitation simulations (Watanabe et al., 2003; Zhang et al., 2006), this means the RANS equations have no problem on accurately obtaining pressure solutions and capture such low pressure and phase changing. It has been shown in the literature that RANS has been successfully applied to predict the risk of cavitation occurring. For instance, Lu et al. (2012) applied RANS to investigate the cavitating flow on a marine propeller. Upon comparison against experiments, they found that RANS has captured the occurrence of the root cavitation, despite that the evolution of cavitation was only partially simulated. For the above reason, RANS is still reckoned as the most productive approach for cavitation modelling.

RANS may be applied as an indicator of whether or not a cavitation phenomenon should appear, while a higher-order approach (Hybrid, LES) is still required to study the changes in ship characteristics due to the presence of cavitation. RANS was found to neglect bubble phenomena that are common in cavitation, as shown in Figure 21. This can be certainly attributed to the time-averaging processing of RANS. This was confirmed by Bensow (2011), who provided a comparison between LES, DDES and RANS on modelling the cavitation vapour generated within the wake of a foil as shown in Figure 22. The figure confirms that

682 RANS fails in simulating the detailed vapour, while LES and DDES are both capable of such modelling,
683 with LES presenting more detailed small-scale vapours than DES.

684

685

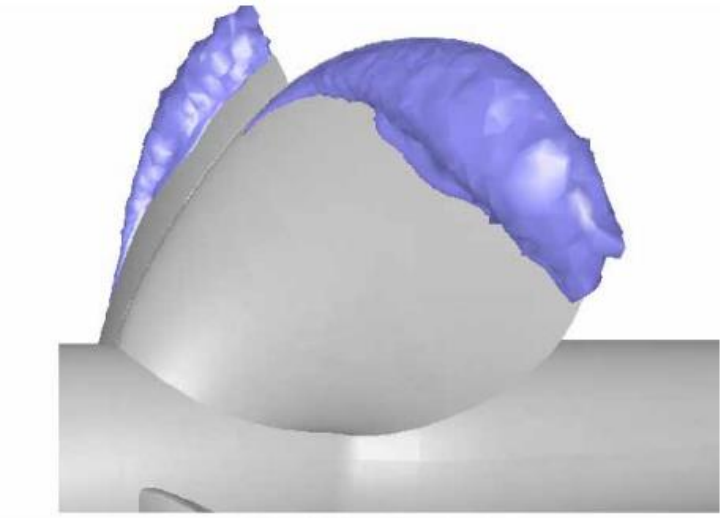

(a) CFD simulation

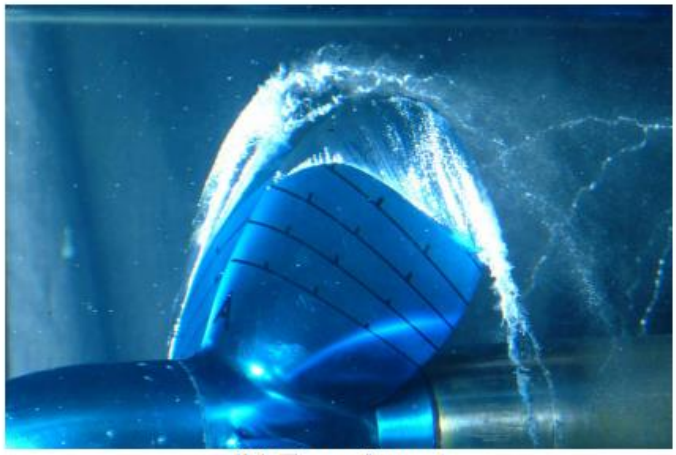

(b) Experiment

686

687 Figure 21: Cavity bubbles generated by rotating blades: a comparison between RANS and experimental.
688 (Watanabe et al., 2003)

689

690

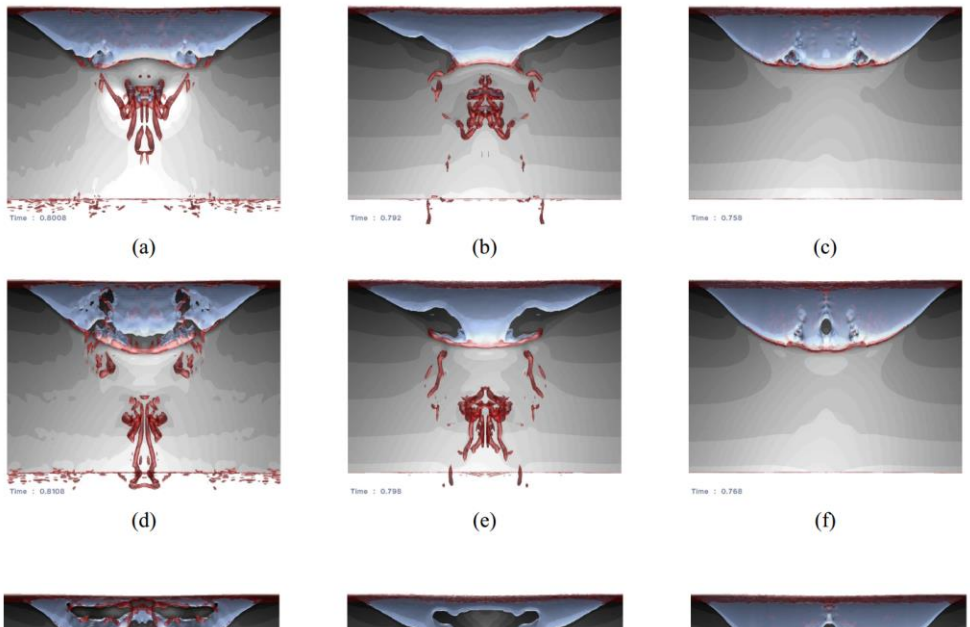

691

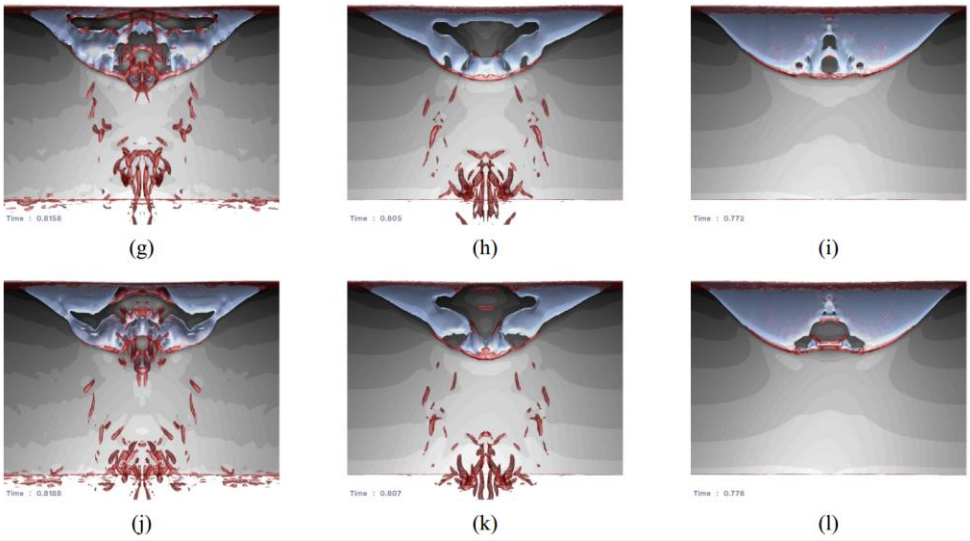

692

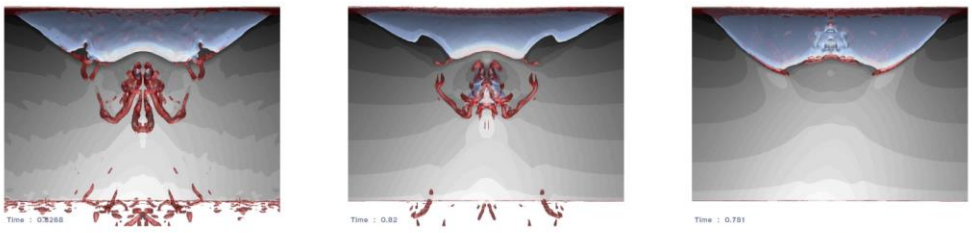

693 Figure 22: Simulation of cavitation on the Delft Twist11 foil: a comparison between LES (left column),
694 DDES (middle column), and RANS (right column). (Bensow, 2011)

695

Viitanen et al. (2018) used DDES to simulate the cavitation patterns generated by propellers and provided a comparison against experiments. Their results are presented in Figure 23 in which cavitation is seen to be exceptionally replicated. The superiority of the DDES hybrid approach is demonstrated for cavitation assessments.

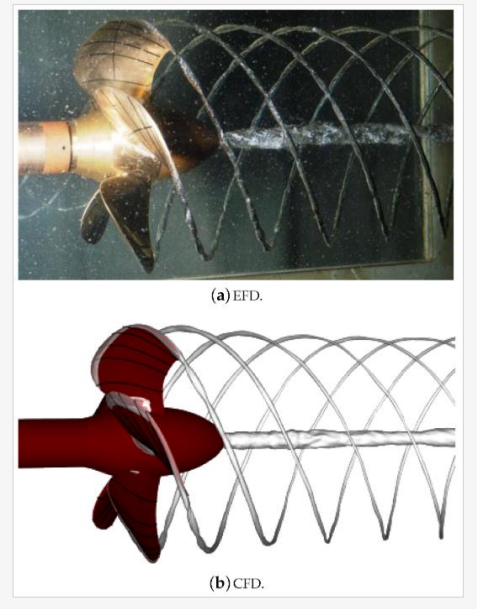

Figure 23: Tip and hub vortex structures during (a) experiments and (b) DDES computations. (Viitanen et al., 2018)

Cavitation is an important factor to cause erosions on ship propeller blades, as it can cause severe damages, erosions and noise. Therefore, accurately modelling propeller erosion demonstrates that it is of great importance that the selected turbulent modelling strategy captures vapour bubbles. This fact remarks on the unsuitability of RANS for erosion predictions. Ponkratov (2015) conducted erosion studies on a full-scale self-propelled ship using DES. The results from their numerical assessments were compared to borescopes observations and underwater propeller inspections. The author reported that CFD underpredicted the development of the tip vortex. This phenomenon was attributed to an under the mesh definition, which was not considered fine enough. However, the numerical model was able to predict cavitation bubbles collapse on the blade surfaces accurately. Therefore, the authors considered their DES model able to accurately predict the propeller erosion areas as confirmed by comparison with underwater propeller inspection results.

Usta et al. (2017) studied ship propellers erosion caused by cavitation using a DES approach and provided a comparison with experiments showing promising capabilities of DES on predicting the erosion damage.

On the other hand, a more accurate way to represent erosion could be by investigating localised turbulent flows using an LES approach. Mahesh et al. (2015) performed LES simulations on ships' three important phenomena: crash-back, cavitation, and hydro-acoustics. Following validation against experiments, the authors demonstrated that the turbulent behaviours within the phenomena can be accurately captured by LES. They also showed RANS are defeated by LES in those tests.

Crashback is an off-design condition in which the marine vessel moves in the forward direction, whereas the propeller rotates in the reverse direction, yielding negative thrust. Flow around the propeller in crashback is characterised by large-scale unsteadiness and flow separation. High amplitude off-axis forces and moments are produced by this unsteadiness, which is transmitted to the body, adversely affecting its manoeuvrability and causing damage and reduction in the performance of propeller blades (Mahesh et al., 2015). Jang and Mahesh (2013) presented the forces of crashback on a ship propeller in the frequency domain, as in Figure 24, alongside validation showing the superb capability of LES on reproducing the unsteady process, especially the low-frequency forces due to flow separation. Wang et al. (2009) assessed the noise caused by a foil, also showing LES can accurately predict the unsteady flow at a frequency-domain level, as shown in Figure 25.

Moreover, Liefvendahl (2010) demonstrated that LES can provide the essential fluid instability within propeller flows, important for noise estimate, and such information would be ignored by RANS' averaging nature. More examples of LES simulations can be found as assessing unsteady force during crash-back (Verma, Jang and Mahesh, 2012; Jang and Mahesh, 2013), cavitation (Bensow and Bark, 2010; Dittakavi et al., 2010; Gnanaskandan and Mahesh, 2015; Lu et al., 2014), and noise (Wang and Moin, 2000).

Following the discussion about, LES has been widely applied to localise ship design. It proves capable of capturing desired information, and those simulations are achievable with a cell number at a level of 10^7 to mesh a specific ship component (Liefvendahl et al., 2010). However, considering multiple components in a larger scale will significantly increase the computational cost and lead LES to be an unaffordable approach, limiting the applicability of standalone LES, because the interactions between multiple components could be essential (Benites-Munoz et al., 2020). In this context, the hybrid method, that allows the simulation of multiple components/zones with different fidelities, is feasible to model a larger ship part using local refinements at key locations.

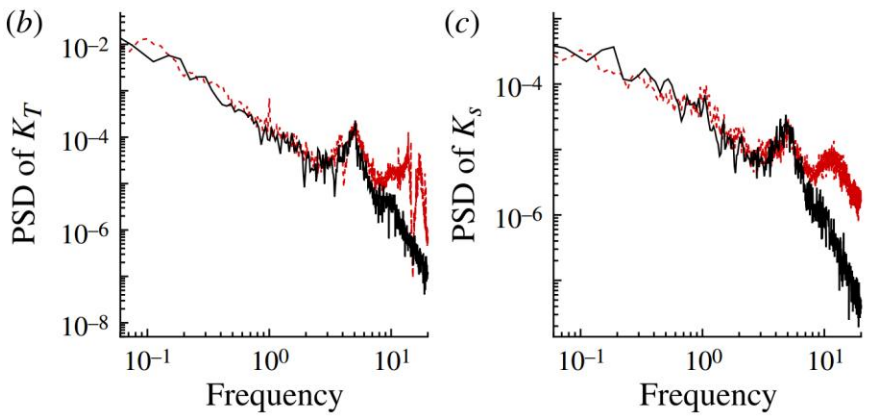

746

747 Figure 24: Validation of thrust coefficient (left) and side-force coefficient (right) in the frequency domain.
748 Solid line: LES; dash line: experimental. (Jang and Mahesh, 2013)

749

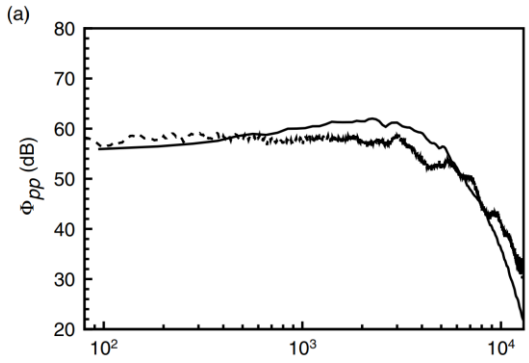

750

751 Figure 25: Frequency spectra of pressure fluctuations on the suction side. Solid line: LES; dash line:
752 experimental. (Wang et al., 2009)

753

754 **4. Discussion**

755 RANS, as illustrated by multiple sources above, neglects the unsteady flow features. This lies in the
756 averaging nature of its mathematical formulation, as shown in Equations (4) and (5). However, RANS
757 proved to provide sufficient accuracy in resistance predictions wake (thus wave-making resistance) and
758 vessels' motions. This essentially means RANS can accurately predict the total hydrodynamic loads of a
759 ship. As expressed in Equation (12), the hydrodynamic load on a ship is integrated of pressure and viscous
760 force on its surface mesh.

761

$$\mathbf{F_h} = \int (-\bar{p}\,\mathbf{n} + \bar{\tau}\cdot\mathbf{n})\,dS \tag{12}$$

762

763 The hydrodynamic force then subsequently governs the motions of a ship, if the ship is not fixed. This can
764 be considered as the combination of translation and rotation, which was solved with the rigid-body motion
765 equations in the body-fixed system based on the mass centre of the ship G-*x'y'z'*, as expressed in Equation
766 (13) and (14) (Huang and Thomas, 2019). This is to say, if pressure and viscous terms are solved correctly
767 as in the RANS equations, plus an appropriate dynamic mesh is applied, they should integrate into a correct
768 hydrodynamic force, e.g. resistance, despite it is an averaged value for each timestep. This, on the other
769 hand, corroborated why mesh convergence is so important.

770

$$\mathbf{F} = m\frac{d\overrightarrow{V_G}}{dt} \tag{13}$$

$$\mathbf{T} = [J]\cdot\frac{d\overrightarrow{\omega_G}}{dt} + \overrightarrow{\omega_G}\times([J]\cdot\overrightarrow{\omega_G}) \tag{14}$$

771

772 where **F** and **T** are the total force and torque on the ship, induced by the gravity, the hydrodynamic load
773 from the surrounding fluid $\mathbf{F_h}$; m and [J] are the mass and inertia moment tensor respectively, and V_G and
774 ω_G are the translational and rotational velocity vectors of the ship respectively.

775 In line with these features, previous studies have demonstrated that RANS models can accurately obtain
776 ship resistance and motions in various situations. This conclusion has been supported by extensive model
777 tests. Among mainstream RANS options, the $k-\omega$ SST scheme is the most favoured and validated one.
778 For full scale, the derivation of formulae from model tests usually needs to apply the ITTC extrapolation
779 procedure since it is impossible to ensure Froude and Reynolds numbers are both equal between full scale
780 and model scale, in which, the former governs gravity/inertia (waves) forces and the latter dictates viscous
781 forces. This procedure divides the total ship resistance into a wave component and a friction component.
782 Scaling based on a consistent Froude number is practical in model tests, which scales the wave component
783 correctly while bringing about certain errors within the friction component due to a changed Reynolds
784 number. The latter may be corrected using the ITTC correlation method (ITTC, 2008).

Directly simulating ship performance in full scale is applicable, as it does not conflict with the CFD theories. Full-scale simulations will make the ITTC extrapolation procedure unnecessary, thus simplifying the procedure of resistance prediction. Moreover, it can solve the boundary layer issues associated with a changed Reynolds number and remain the correct scale's fluid behaviours. However, due to a lack of full-scale sea trial data, this has not been fully validated and will need years of a process. Preliminary results have shown to be promising (Lloyds Register, 2016), which gives confidence in RANS. Considering the mathematic roots, model-scale validations and full-scale validations, this review proposes that RANS can provide sufficiently accurate resistance predictions and there is not much room for improvement from applying more complex turbulence modelling strategies, i.e. RANS is the fastest and cheapest approach to predict ship resistance.

On the other hand, as the statistically time-averaging process within RANS ignores certain fluid instabilities, important physics might be oversimplified in certain scenarios. This caused RANS to be proved incapable of applications where fluid instabilities are significant, such as structural vibration and noise predictions. Meanwhile, the relatively coarse mesh of RANS has been shown to introduce inaccuracies to small vortex structures, important within propeller flows. These incapabilities have limited the application of RANS to assessing integrated ship performance. Thus, RANS suitability depends on the problem of investigation, e.g. integrate or local, steady or unsteady; and based on its certain inapplicability, there is a need to use higher-order turbulent strategies to simulate such problems. It has been a trend that RSM models can remedy the rough flow features predicted by eddy-viscosity based RANS; however, RSM has to date much less applied to ship hydrodynamic simulations. DNS, on the other hand, could allow the modelling of more complex flows. Yet, DNS has no practicality for the simulation of ship viscous flows in the near future. Moreover, the numerical order of magnitude of mesh and timestep requirements makes DNS a huge numerical task and remains unlikely to be achieved in practice. Thus DNS is more suitable for relatively pure fluid dynamic analyses. Also, as a cheaper solution than DNS, LES has proved to provide sufficient accuracy in complex ship design applications.

LES allows the modelling of complex flow features that RANS inherently neglects. It was shown to be very accurate in predicting detailed ship flow behaviours, able to capture the instabilities ignored by RANS. Thus, LES could be successfully applied to the assessment of structural vibration, noise, and erosion. Multiple publications even used frequency spectrums to demonstrate the excellence of LES. However, the main disadvantage of using LES is the requirement of very fine grids in the near-wall regions of the flow domain and a minimal timestep size. Consequently, pure LES applicability for the simulation of an entire hull is deemed far from reality in the industry. The literature has demonstrated that LES is currently just applied to localised simulations limited to a specific component's scale, such as a propeller. Thus, LES has

still been deemed an unaffordable approach for scenarios where interactions between ship components are important.

Hybrid turbulence modelling strategies based on the combination of RANS and LES techniques are becoming increasingly popular in ship hydromechanics. They have the inherent ability to predict well highly unsteady and separated flows while their mesh requirements are lower than LES. Also, they tend to present fewer convergence issues than RSM and be less sensitive to inlet boundary conditions. One of the main applications where hybrid DES approaches have shown clear superiority is for the prediction of local flows, ship boundary layers and wakes when flow separation is expected. Therefore, it is recommended to use a hybrid approach for simulating flows for propellers, rudder loading, energy-saving devices, and any other applications where boundary layer and wake flows need to be assessed in detail.

However, there are two important challenges for hybrid DES approaches. First, the transition between RANS and LES reckons to be the main obstacle of DES. One of the consequences is that there is a high risk from the grid point of view that the simulation can act in RANS mode in the targeted LES region. In the same line, the supposed LES zone might end up being treated as RANS. This phenomenon happens if no special care is taken while meshing, which might hinder hybrid models' popularisation. Even with the most advanced DES approach, the IDDES still shows incapable of addressing physical abnormalities present in the formulation. Therefore, it is clear that more computational developments are expected to avoid the grey area issues present in contemporary IDDES approaches. Secondly, more advanced DES models need still to be validated for the simulation of ship viscous flows. Other DES approaches have already demonstrated their superiority for the simulation of viscous flows in industrial applications. For example, ZDES (Zonal Detached Eddy Simulations) allows the CFD user to define the RANS and LES zones, but this approach has not been validated for ship viscous flow applications yet. Therefore, a CFD user intending to implement hybrid approaches should always check that the targeted RANS/LES zones are actually treated as RANS/LES in the CFD software before accepting the results obtained from the run.

An alternative approach, WMLES may offer significant advantages when compared to wall-resolving LES. As demonstrated by Liefvendahl and Johansson (2021), WMLES is excellent for modelling detailed ship hydrodynamics and meanwhile offers a substantial mesh saving when compared to a pure wall-resolving LES approach. However, WMLES techniques also present challenges and may provide numerical inaccuracies such as the log-layer mismatch. According to Larsson et al. (2016), in WMLES, the height of the wall-modelled region should be carefully chosen as this parameter directly impact the mesh resolution and modelled results; An inappropriate selection may cause the wall shear stress to be under/overpredicted,

influencing the modelling of flow details such as separation. Besides, WMLES simulations are expected to have higher computational costs than DES simulations.

In general, DES and WMLES (both of them model the near-wall region) are still under development and being studied for marine applications. They are more expensive than RANS, although cheaper than Wall-Resolved LES. It is expected that the errors and inaccuracies of these models may be corrected in a near future. An enhanced practice on local mesh refinement may also speed up this popularisation (Jasak et al., 2019). In addition, developments in data-driven CFD (Pena et al., 2020c; Pena and Huang, 2021) could make the DES set-up task semiautomatic. This would make high-order turbulence modelling approaches more accessible for the ship hydrodynamic CFD community.

In the present discussion, decision-making mainly involves making decisions considering the compromise between turbulent fidelity and computational costs. It is worth noting that such difference in computational costs lies in mesh requirement, specifically, the precise level of the modelling boundary layer, reflecting the Y^+ value. Thus, it has been a consensus that RANS simulations can provide accurate results with a Y^+ of 100, while that shall be 1 for LES (ITTC, 2014a; Arslan et al., 2016), and the Hybrid approach has different requirements in the RANS region and the LES region respectively. This determines the mesh density around the hull geometry. As numerical divergence will occur when the expansion ratio between mesh layers is too high (a ratio of less than 1.25 is recommended), the cell thickness can only gradually increase layer-by-layer from the geometry surface towards the whole computational domain. Thus, the limitation of boundary layer geometry will cost the computational cells to change as a whole. On the other hand, denser mesh shall be matched by a smaller timestep. This relationship lies in the definition of Courant number (Co):

$$\mathrm{Co} = \frac{\mathrm{u}\Delta\mathrm{t}}{\Delta\mathrm{x}} \tag{15}$$

where $\Delta\mathrm{t}$ is the timestep size, $\mathrm{u}/\Delta\mathrm{x}$ is its normal velocity divided by the distance between the cell centre and the centre of the neighbour cell. To avoid numerical convergency, the Co value should be restricted for different applications, such as less than 1 for relative mild flows and less than 0.3 breaking type flows (Huang et al., 2019, 2021c). Therefore, the turbulence modelling strategy selection will dictate y^+ then link to overall mesh density and timestep choices, thus enormously influencing the computational costs.

Thereafter, the recommendations of the present work will be made based on two principles:

879 (a) the purpose of the specific ship-design task can be done, and the accuracy should be acceptable.

880 If principle (a) is satisfied:

881 (b) using as cheap a turbulence modelling strategy as possible, here meaning the least mesh requirement.

882 Based on this paper's review and discussion, the recommendation of turbulence strategies for various ship
883 hydrodynamic simulations is given in Table 1.

884

885

886

887

888

889

890

891

892

893

894

895

896

897

898

899

900

901

902

903 Table 1: Applicability summary and recommendations of turbulence modelling strategies.

904

Applications	**Recommending turbulence strategy**	**Mesh estimation**	**Y+**	**Maturity and accuracy (deviation against measurements)**
Ship resistance/motions	RANS	Model scale: 1-5 million (Zha et al., 2014a; Dashtimanesh et al., 2020) Full scale: 5-10 million (Tezdogan et al., 2015)	30-100	Mature technology, less than 10% deviation
Boundary layer flow	DES	Model scale: 10-25 million (Kornev et al., 2018) Full-scale: ~50 million (Pena et al., 2019)	0-5	Early Technology, has shown great accuracy
Self-propulsion (only predict integrated thrust and torque coefficients)	RANS + virtual/actuator disc approach	Model scale 5-10 million (Tokyo 2015 Workshop) Full-scale: 5-20 million (Jasak et al., 2019)	30-100	Mature technology, less than 10% deviation
Self-propulsion (for local flow analysis with insignificant flow separation)	RANS with fully discretised propeller	Model scale: 5-10 million (Kornev and Abbas, 2018) Full scale: 5-20 million (Sun et al, 2020)	30-100	Mature Technology Less than 10% deviation
Self-propulsion (for local flows with significant flow separation)	DES with fully discretised propeller	Model scale 5-10 million (Kornev and Abbas, 2018) Full-scale: ~50 million (Pena et al., 2019)	0-5	Early Technology has shown great accuracy
Cavitation (only predict occurance)	RANS	~2 million (Lu et al., 2012)	30-100	Mature technology, Can predict whether or not a cavitation phenomenon should appear, but cannot predict the changes in ship characteristics due to the presence of cavitation
Cavitation (full flow behaviours)	LES	20 - 100 million (Mahesh et al., 2015)	0-5	Mature technology, while the development of DES can potentially reduce the computational cost
Component vibration/noise/ damage	LES	5-20 million (Wang et al., 2009; Jang and Mahesh, 2013)	0-5	Mature technology, very accurate and validated in a frequency-domain level

905

906

5. Conclusions

This paper has analysed primary turbulence modelling strategies' capability, limitation, computational cost, and accuracy for various ship hydrodynamic applications, providing a turbulence modelling selection recommendation based on the findings. The work has the potential to serve as an up-to-date guideline for ship hydrodynamic simulations, as well as facilitating a wider CFD community in terms of turbulence modelling.

In summary, RANS shows excellent capabilities in predicting the integral performance of a ship such as forces and moments in both model scale and full scale. However, RANS omits certain details of the flow, which typically causes inaccuracies when assessing ship performance related to detailed flow velocity and vorticity. The detailed flow features can be effectively modelled using LES, but this method is only cost-effective to study a small-scale problem that does not cover a large part of a ship (e.g. studying propeller cavitation), as larger-scale LES simulations are still prohibitively expensive. On the other hand, the WMLES approach and the hybrid DES approach are shown promising to model high-fidelity flows whilst keeping the computational cost affordable, but both approaches are harder to use than RANS or LES because they remain certain numerical challenges that are very sensitive to setups. With experience being gained, WMLES and DES are expected to develop into mature alternatives to RANS and LES.

References

Arslan, T., Pettersen, B., Andersson, H.I., 2016. Large-eddy simulation of cross-flow around ship sections. Journal of Marine Science and Technology 21, 552–566.

ASME, 2009. Verification & Validation in Computational Fluid Dynamics & Heat Transfer [WWW Document]. URL https://www.asme.org/codes-standards/find-codes-standards/v-v-20-standard-verification-validation-computational-fluid-dynamics-heat-transfer (accessed 2.21.20).

Bakica, A., Vladimir, N., Gatin, I., Jasak, H., 2020. CFD simulation of loadings on circular duct in calm water and waves. Ships and Offshore Structures 1–13.

Benites-Munoz, D., Huang, L., Anderlini, E., Marín-Lopez, J.R., Thomas, G., 2020. Hydrodynamic Modelling of An Oscillating Wave Surge Converter Including Power Take-Off. Journal of Marine Science and Engineering 8, 771.

Bensow, R.E., 2011. Simulation of the unsteady cavitation on the Delft Twist11 foil using RANS, DES and LES, in: Second International Symposium on Marine Propulsors, Hamburg, Germany.

Bensow, R.E., Bark, G., 2010. Implicit LES predictions of the cavitating flow on a propeller. Journal of Fluids Engineering.

Bhushan, S., Carrica, P., Yang, J., Stern, F., 2011. Scalability and validation study for large scale surface combatant computations using CFDShip-Iowa. The International Journal of High Performance Computing Applications 25, 466–487.

Carrica, P.M., Fu, H., Stern, F., 2011. Computations of self-propulsion free to sink and trim and of motions in head waves of the KRISO Container Ship (KCS) model. Applied Ocean Research 33, 309–320. https://doi.org/10.1016/j.apor.2011.07.003

Cha, R., Wan, D., 2015. Numerical investigation of motion response of two model ships in regular waves. Procedia engineering 116, 20–31.

Constantinescu, G., Chapelet, M., Squires, K., 2003. Turbulence modeling applied to flow over a sphere. AIAA Journal 41, 1733–1742. https://doi.org/10.2514/2.7291

Dashtimanesh, A., Tavakoli, S., Kohansal, A., Khosravani, R., Ghassemzadeh, A., 2020. Numerical study on a heeled one-stepped boat moving forward in planing regime. Applied Ocean Research 96, 102057.

Deng, G.B., Queutey, P., Visonneau, M., 2005. Three-dimensional flow computation with Reynolds stress and algebraic stress models, in: Engineering Turbulence Modelling and Experiments 6. Elsevier, pp. 389–398.

Dittakavi, N., Chunekar, A., Frankel, S., 2010. Large eddy simulation of turbulent-cavitation interactions in a venturi nozzle. Journal of Fluids Engineering.

ATKINS and VIRTUE. Best Practice Guidelines for the application of Computational Fluid Dynamics in Marine Hydrodynamics. Tech. rep., VIRTUE-The Virtuel Tank Utility in Europe.

Ferziger, J.H., Perić, M., Street, R.L., 2002. Computational methods for fluid dynamics. Springer.

Gnanaskandan, A., Mahesh, K., 2015. A numerical method to simulate turbulent cavitating flows. International Journal of Multiphase Flow.

Guilmineau, E., Deng, G.B., Leroyer, A., Queutey, P., Visonneau, M., Wackers, J., 2018. Assessment of hybrid RANS-LES formulations for flow simulation around the Ahmed body. Computers & Fluids 176, 302–319.

Hanjalić, K., Launder, B., 2009. Modelling turbulence in engineering and the environment: Second-moment routes to closure. https://doi.org/10.1017/CBO9781139013314

Hino, T., Stern, F., Larsson, L., Visonneau, M., Hirata, N., Kim, J., 2020. Numerical Ship Hydrodynamics: An Assessment of the Tokyo 2015 Workshop. Springer Nature.

Huang, L., Li, M., Romu, T., Dolatshah, A., Thomas, G., 2021a. Simulation of a ship operating in an open-water ice channel. Ships and Offshore Structures 16, 353–362. https://doi.org/10.1080/17445302.2020.1729595

Huang, L., Li, Z., Ryan, C., Ringsberg, J.W., Pena, B., Li, M., Ding, L., Thomas, G., 2021b. Ship resistance when operating in floating ice floes: Derivation, validation, and application of an empirical equation. Marine Structures 79, 103057.

Huang, L., Ren, K., Li, M., Tuković, Ž., Cardiff, P., Thomas, G., 2019. Fluid-structure interaction of a large ice sheet in waves. Ocean Engineering 182, 102–111.

Huang, L., Tavakoli, S., Li, M., Dolatshah, A., Pena, B., Ding, B., Dashtimanesh, A., 2021c. CFD analyses on the water entry process of a freefall lifeboat. Ocean Engineering 232, 109115.

Huang, L., Thomas, G., 2019. Simulation of Wave Interaction With a Circular Ice Floe. Journal of Offshore Mechanics and Arctic Engineering 141, 041302.

Huang, L., Tuhkuri, J., Igrec, B., Li, M., Stagonas, D., Toffoli, A., Cardiff, P., Thomas, G., 2020. Ship resistance when operating in floating ice floes: A combined CFD&DEM approach. Marine Structures 74, 102817.

ITTC, 2017. Benchmark Database for CFD Validation for Resistance and Propulsion. Recommended Procedures and Guidelines.

ITTC, 2014a. Guidelines: Practical Guidelines for Ship CFD Applications. ITTC Report.

ITTC, 2014b. 27th Propulsion Committee Proceedings. ITTC Report.

ITTC, 2008. 1978 ITTC Performance Prediction Method. Recommended Procedures and Guidelines.

ITTC, 1957. ITTC Proceedings of the 8th International Conference, in: 8th ITTC Conference.

Jang, H., Mahesh, K., 2013. Large eddy simulation of flow around a reverse rotating propeller. Journal of Fluid Mechanics.

Jasak, H., Jemcov, A., Tukovic, Z., 2007. OpenFOAM: A C++ library for complex physics simulations, in: International Workshop on Coupled Methods in Numerical Dynamics. IUC Dubrovnik, Croatia, pp. 1–20.

Jasak, H., Vukčević, V., Gatin, I., Lalović, I., 2019. CFD validation and grid sensitivity studies of full scale ship self propulsion. International Journal of Naval Architecture and Ocean Engineering 11, 33–43.

Khojasteh, D., Tavakoli, S., Dashtimanesh, A., Dolatshah, A., Huang, L., Glamore, W., Sadat-Noori, M., Iglesias, G., 2020. Numerical analysis of shipping water impacting a step structure. Ocean Engineering 209, 107517.

Kolmogorov, A.N., 1941. The Local Structure of Turbulence in Incompressible Viscous Fluid for Very Large Reynolds Numbers. Proceedings of the Royal Society A: Mathematical, Physical and Engineering Sciences 434, 9–13. https://doi.org/10.1098/rspa.1991.0075

Kornev, N., Abbas, N., 2018. Vorticity structures and turbulence in the wake of full block ships. Journal of Marine Science and Technology 23, 567–579.

Kornev, N., Shevchuk, I., Abbas, N., Anschau, P., Samarbakhsh, S., 2019. Potential and limitations of scale resolved simulations for ship hydrodynamics applications. Ship Technology Research 66, 83–96. https://doi.org/10.1080/09377255.2019.1574965

Kornev, N., Taranov, A., Shchukin, E., Kleinsorge, L., 2011. Development of hybrid URANS-LES methods for flow simulation in the ship stern area. Ocean Engineering 38, 1831–1838. https://doi.org/10.1016/j.oceaneng.2011.09.024

Larsson, J., Kawai, S., Bodart, J., Bermejo-Moreno, I., 2016. Large eddy simulation with modeled wall-stress: recent progress and future directions. Mechanical Engineering Reviews 3, 15–00418.

Larsson, L., Stern, F., Visonneau, M., 2013. Numerical ship hydrodynamics: an assessment of the Gothenburg 2010 workshop. Springer.

Larsson, L., Stern, F., Visonneau, M., Hino, T., Hirata, N., Kim, J., 2015. Proceedings, Tokyo 2015 Workshop on CFD in Ship Hydrodynamics.

Leonard, A., 1975. Energy cascade in large-eddy simulations of turbulent fluid flows, in: Advances in Geophysics. Elsevier, pp. 237–248.

Liefvendahl, M., 2010. Investigation of propeller wake instability using LES. Ship Technology Research 57, 100–106.

Liefvendahl, M., Alin, N., Chapuis, M., Fureby, C., Svennberg, U., Troëng, C., 2010. Ship and propulsor hydrodynamics, in: V European Conference on Comput. Fluid Dynamics.

Liefvendahl, M., Fureby, C., 2017. Grid requirements for LES of ship hydrodynamics in model and full scale. Ocean Engineering 143, 259–268. https://doi.org/10.1016/j.oceaneng.2017.07.055

Liefvendahl, M., Johansson, M., 2021. Wall-modeled LES for ship hydrodynamics in model scale. Journal of Ship Research 65, 41–54.

Lloyds Register, 2016. Workshop on Ship Scale Hydrodynamic Computer Simulation Proceedings.

Lu, N.X., Bensow, R.E., Bark, G., 2014. Large eddy simulation of cavitation development on highly skewed propellers. Journal of Marine Science and Technology 19, 197–214.

Lu, N.X., Svennberg, U., Bark, G., Bensow, R., 2012. Numerical simulations of the cavitating flow on a marine propeller, in: 8th International Symposium on Cavitation.

Mahesh, K., Kumar, P., Gnanaskandan, A., Nitzkorski, Z., 2015. LES applied to ship research. Journal of Ship Research 59, 238–245.

McComb, W.D., 1990. The physics of fluid turbulence. Chemical physics.

Menter, F.R., Kuntz, M., 2004. Adaptation of Eddy-Viscosity Turbulence Models to Unsteady Separated Flow Behind Vehicles 339–352. https://doi.org/10.1007/978-3-540-44419-0_30

Mikkelsen, H., Walther, J.H., 2020. Effect of roughness in full-scale validation of a CFD model of self-propelled ships. Applied Ocean Research 99, 102162.

Mucha, P., Deng, G., Gourlay, T., Moctar, O., 2016. Validation studies on numerical prediction of ship squat and resistance in shallow water, in: 4th MASHCON-International Conference on Ship Manoeuvring in Shallow and Confined Water with Special Focus on Ship Bottom Interaction. pp. 122–133.

Nikitin, N. V., Nicoud, F., Wasistho, B., Squires, K.D., Spalart, P.R., 2000. An approach to wall modeling in large-eddy simulations. Physics of Fluids 12, 1629–1632. https://doi.org/10.1063/1.870414

Nishikawa, T., Yamade, Y., Sakuma, M., Kato, C., 2012. Application of fully-resolved large eddy simulation to KVLCC2. Journal of the Japan Society of Naval Architects and Ocean Engineers 16, 1–9.

Paterson, E.G., Wilson, R. V., Stern, F., 2003. General-purpose parallel unsteady rans ship hydrodynamics code: Cfdshipiowa., IIHR Report 432. Iowa Institute for Hydraulic Research. The University of Iowa, Iowa, USA.

Pena, B., Huang, L., 2021. Wave-GAN: A deep learning approach for the prediction of nonlinear regular wave loads and run-up on a fixed cylinder. Coastal Engineering 103902.

Pena, B., Muk-Pavic, E., Fitzsimmons, P., 2020a. Detailed analysis of the flow within the boundary layer and wake of a full-scale ship. Ocean Engineering 218, 108022.

Pena, B., Muk-Pavic, E., Ponkratov, D., 2019. Achieving a high accuracy numerical simulations of the flow around a full scale ship, in: International Conference on Offshore Mechanics and Arctic Engineering. American Society of Mechanical Engineers, p. V07AT06A058.

Pena, B., Muk-Pavic, E., Thomas, G., Fitzsimmons, P., 2020b. An approach for the accurate investigation of full-scale ship boundary layers and wakes. Ocean Engineering 214, 107854.

Pena, B., Huang, L., Ahlgren, F., 2020c. A Review on Applications of Machine Learning in Shipping Sustainability, in: SNAME Maritime Convention. The Society of Naval Architects and Marine Engineers.

Ponkratov, D., 2017. Proceedings: 2016 Workshop on Ship Scale Hydrodynamic Computer Simulations. Lloyd's Register, Southampton, United Kingdom.

Ponkratov, D., Zegos, C., 2015. Validation of ship scale CFD self-propulsion simulation by the direct comparison with sea trials results, in: Proceedings of the Fourth International Symposium on Marine Propulsors.

Pope, S.B., 2001. Turbulent flows. IOP Publishing.

Shen, L., Zhang, C., Yue, D.K.P., 2002. Free-surface turbulent wake behind towed ship models: Experimental measurements, stability analyses and direct numerical simulations. Journal of Fluid Mechanics 469, 89–120. https://doi.org/10.1017/S0022112002001684

Shen, Z., Wan, D., 2013. RANS computations of added resistance and motions of a ship in head waves. International Journal of Offshore and Polar Engineering 23, 264–271.

Shur, M.L., Spalart, P.R., Strelets, M.K., Travin, A.K., 2008. A hybrid RANS-LES approach with delayed-DES and wall-modelled LES capabilities. International Journal of Heat and Fluid Flow 29, 1638–1649. https://doi.org/10.1016/j.ijheatfluidflow.2008.07.001

Smagorinsky, J., 1963. General circulation experiments with the primitive equations: I. The basic experiment. Monthly weather review 91, 99–164.

Smith, T.A., Ventikos, Y., 2021. Wing-tip vortex dynamics at moderate Reynolds numbers. Physics of Fluids 33, 035111.

Song, S., Demirel, Y.K., Atlar, M., 2019. An investigation into the effect of biofouling on the ship hydrodynamic characteristics using CFD. Ocean Engineering 175, 122–137.

Song, S., Demirel, Y.K., Muscat-Fenech, C.D.M., Sant, T., Villa, D., Tezdogan, T., Incecik, A., 2021. Investigating the effect of heterogeneous hull roughness on ship resistance using CFD. Journal of Marine Science and Engineering 9, 202.

Sotiropoulos, F., Patel, V.C., 1995. Application of Reynolds-stress transport models to stern and wake flows. Journal of Ship Research 39, 263–283.

Spalart, P.R., 2009. Detached-Eddy Simulation. Annual Review of Fluid Mechanics 41, 181–202. https://doi.org/10.1146/annurev.fluid.010908.165130

Spalart, P.R., Deck, S., Shur, M.L., Squires, K.D., Strelets, M.K., Travin, A., 2006. A new version of detached-eddy simulation, resistant to ambiguous grid densities. Theoretical and Computational Fluid Dynamics 20, 181–195. https://doi.org/10.1007/s00162-006-0015-0

Spalart, P.R., Jou, W.H., Strelets, M.K., Allmaras, S.R., 1997. Comments on the feasibility of LES for wings and on a hybrid RANS/LES approach. Advances in DNS/LES 1, 4–8.

Sun, W., Hu, Q., Hu, S., Su, J., Xu, J., Wei, J., Huang, G., 2020. Numerical Analysis of Full-Scale Ship Self-Propulsion Performance with Direct Comparison to Statistical Sea Trail Results. Journal of Marine Science and Engineering 8, 24.

Terziev, M., Tezdogan, T., Incecik, A., 2019. Application of eddy-viscosity turbulence models to problems in ship hydrodynamics. Ships and Offshore Structures 1–24.

Tezdogan, T., Demirel, Y.K., Kellett, P., Khorasanchi, M., Incecik, A., Turan, O., 2015. Full-scale unsteady RANS CFD simulations of ship behaviour and performance in head seas due to slow steaming. Ocean Engineering 97, 186–206. https://doi.org/10.1016/j.oceaneng.2015.01.011

Tezdogan, T., Incecik, A., Turan, O., 2016. Full-scale unsteady RANS simulations of vertical ship motions in shallow water. Ocean Engineering 123, 131–145.

Usta, O., Aktas, B., Maasch, M., Turan, O., Atlar, M., Korkut, E., 2017. A study on the numerical prediction of cavitation erosion for propellers. Fifth International Symposium on Marine Propulsion smp'17.

Verma, A., Jang, H., Mahesh, K., 2012. The effect of an upstream hull on a propeller in reverse rotation. Journal of Fluid Mechanics.

Viitanen, V.M., Hynninen, A., Sipilä, T., Siikonen, T., 2018. DDES of wetted and cavitating marine propeller for CHA underwater noise assessment. Journal of Marine Science and Engineering 6. https://doi.org/10.3390/jmse6020056

Wackers, J., Koren, B., Raven, H.C., Van der Ploeg, A., Starke, A.R., Deng, G.B., Queutey, P., Visonneau, M., Hino, T., Ohashi, K., 2011. Free-surface viscous flow solution methods for ship hydrodynamics. Archives of Computational Methods in Engineering 18, 1–41.

Wang, M., Moin, P., 2000. Computation of trailing-edge flow and noise using large-eddy simulation. AIAA Journal.

Wang, M., Moreau, S., Iaccarino, G., Roger, M., 2009. Les prediction of wall-pressure fluctuations and noise of a low-speed airfoil. International Journal of Aeroacoustics.

Watanabe, T., Kawamura, T., Takekoshi, Y., Maeda, M., Rhee, S.H., 2003. Simulation of steady and unsteady cavitation on a marine propeller using a RANS CFD code, in: Proceedings of The Fifth International Symposium on Cavitation (Cav. Citeseer.

Winden, B., Turnock, S.R., Hudson, D.A., 2014. Self-propulsion modelling of the KCS container ship using an open source framework.

Xing, T., Bhushan, S., Stern, F., 2012. Unsteady vortical flow and turbulent structures for a tanker hull form at large drift angles. Ocean Eng 55, 23–43.

Yang, J., Bhushan, S., Suh, J., Wang, Z., Koo, B., Sakamoto, N., Xing, T., Stern, F., 2008. Large-eddy simulation of ship flows with wall-layer models on Cartesian grids, in: Proceedings of 27th Symposium on Naval Hydrodynamics. Seoul, Korea.

Zha, R, Ye, H., Shen, Z., Wan, D., 2014. Numerical study of viscous wave-making resistance of ship navigation in still water. Journal of Marine Science and Application 13, 158–166.

Zha, R, Ye, H., Shen, Z., Wan, D., 2014. Numerical computations of resistance of high speed catamaran in calm water. Journal of Hydrodynamics 26, 930–938.

Zhang, Z., Liu, H., Zhu, S., Zhao, F., 2006. Application of CFD in ship engineering design practice and ship hydrodynamics. Journal of Hydrodynamics 18, 308–315.

Zou, L., Larsson, L., Orych, M., 2010. Verification and validation of CFD predictions for a manoeuvring tanker. Journal of Hydrodynamics, Ser. B 22, 438–445. https://doi.org/10.1016/S1001-6058(09)60233-X